Available online at www.sciencedirect.com
SCIENCE DIRECT®
Sedimentary Geology 167 (2004) 57–89
Sedimentary Geology
www.elsevier.com/locate/sedgeo

Provenance analysis using conglomerate clast lithologies: a case study from the Pahau terrane of New Zealand

Anekant M. Wandres[a,*], John D. Bradshaw[a], Steve Weaver[a], Roland Maas[b], Trevor Ireland[c], Nelson Eby[d]

[a] *Department of Geological Sciences, University of Canterbury, Private Bag 4800, Christchurch, New Zealand*
[b] *Isotope Geochemistry Laboratory, University of Melbourne, Parkville, Victoria 3010, Australia*
[c] *Geochronology and Isotope Geochemistry, Research School of Earth Sciences, The Australian National University, Canberra ACT 0200, Australia*
[d] *Department of Environmental, Earth and Atmospheric Sciences, University of Massachusetts, Lowell, MA 01854, USA*

Received 7 August 2003; received in revised form 30 December 2003; accepted 3 February 2004

Abstract

The field of provenance analysis has undergone a revolution with the development of single-crystal isotope dating techniques using mainly silt to sand sized single minerals. This study focuses on coarser-grained rocks, notably conglomerates, which involve much shorter transport distances and therefore may be used to trace proximal sources. The Torlesse terranes—part of the New Zealand Eastern Province—are accretionary complexes that comprise an enormous volume of quartzofeldspathic sandstones and mudstones with subsidiary conglomerates plus minor oceanic assemblages. Two terranes are recognised in the South Island, the Permian to Late Triassic Rakaia terrane and the Late Jurassic to Early Cretaceous Pahau terrane. Geochronology, geochemistry and Sr–Nd isotopes of igneous clasts from Pahau terrane conglomerates identify the Median Tectonic Zone (s.l.) as a major contributor of detritus to the Pahau depositional basin. SHRIMP U–Pb zircon ages of igneous clasts range from 128 to 123 Ma and from 147 to 135 Ma. Calc-alkaline clasts of the latter range are indistinguishable in age, chemical composition, and petrogenesis from the calc-alkaline granitoids of the Darran Suite, whereas alkaline clasts correlate with the Electric Granite, both parts of the Median Tectonic Zone. An Early Jurassic calc-alkaline rhyolite clast from Kekerengu (188 ± 3 Ma) correlates with the Bounty Island Granite, Campbell Plateau. The petrography and geochemistry of Pahau terrane sandstone clasts indicate the recycling of Permian to early Late Triassic older Rakaia terrane rocks. This is further supported by the detrital zircon age data. Igneous conglomerate clasts are capable of placing exceptionally tight constraints on Pahau provenance and on its Mesozoic tectonic setting within the Southwest Pacific margin of Gondwana. They provide the best evidence yet that the Pahau terrane is locally derived.

Keywords: Provenance; Conglomerate clast; Geochronology; Isotope chemistry; Pahau terrane; Rakaia terrane; New Zealand; Median Tectonic Zone; Antarctica; Marie Byrd Land; Amundsen Province

* Corresponding author. Tel.: +64-3-364-2700; fax: +64-3-364-2769.
E-mail addresses: anekant.wandres@canterbury.ac.nz (A.M. Wandres), john.bradshaw@canterbury.ac.nz (J.D. Bradshaw), steve.weaver@canterbury.ac.nz (S. Weaver), maasr@unimelb.edu.au (R. Maas), Trevor.Ireland@anu.edu.au (T. Ireland), Nelson_Eby@uml.edu (N. Eby).

0037-0738/$ - see front matter © 2004 Elsevier B.V. All rights reserved.
doi:10.1016/j.sedgeo.2004.02.002

1. Introduction

Over the last two decades, the field of provenance analysis has undergone a revolution with the development of single-crystal isotope dating techniques. Many attempts were made to determine the provenance of sedimentary rocks using silt to sand sized single minerals (Adams and Kelley, 1998; Cawood et al., 1999; Ireland, 1992; Ireland et al., 1998; Pell et al., 1997; Pickard et al., 2000; Sircombe, 1999). Fine sand and shale-size sediment may be transported over thousands of kilometres (Pell et al., 1997; Sircombe, 1999), with potential problems for provenance studies (e.g., Bassett, 2000). In this study, we have focused on coarser-grained rocks, notably conglomerates, which involve much shorter transport distances (tens to hundreds of kilometres, Ferguson et al., 1996; Kodama, 1994) and therefore may be used to trace proximal sources.

Sandstones and mudstones of the Late-Permian to Early Cretaceous Torlesse sediments underlie approximately 60–70% of the New Zealand land area and a large part of the New Zealand micro-continent (Fig. 1 (Moore et al., 1982)). In the South Island, Torlesse sediments are recognised in two terranes, the Permian to Late Triassic Rakaia terrane and the Late Jurassic to Early Cretaceous Pahau terrane (Fig. 2). These two terranes are separated by the Esk Head Melange (Bradshaw, 1973; Silberling et al., 1988). Recent studies of Torlesse depositional and deformational environments have recognised similarities with other large sandstone-dominated accretionary complexes in the circum-Pacific region, notably the Franciscan Complex in California and sandstone belts in Alaska, Japan and Antarctica. Consequently, a submarine fan depositional model and an accretionary wedge deformational model are now favoured for the Torlesse (Andrews et al., 1976; Bradshaw et al., 1981; George, 1992; Howell, 1980; Mazengarb and Harris, 1994).

It is widely accepted that the Torlesse terranes have formed along Gondwana's Panthalassan plate margin, which constitutes one of the most extensive orogenic belts in Earth history. Originally established during Neoproterozoic rifting, the margin became a long-lived subduction zone during early Paleozoic convergent tectonism (e.g., Floettmann et al., 1993). Subsequent accretion of arc-trench systems, and possibly micro-continental fragments, formed a series of eastward-migrating orogenic belts: the formerly continuous Neoproterozoic–Ordovician Ross and Delamerian Orogens (e.g., Coney et al., 1990; Floettmann et al., 1993; Stump et al., 1986), the Cambrian–Carboniferous Lachlan and Thompson Orogens (e.g., Coney et al., 1990; Foster and Gray, 2000), and the Silurian–Cretaceous New England Fold Belt (e.g., Powell and Li, 1994). Remnants of these orogenic belts are preserved in the formerly contiguous Gondwana fragments of Australia, Antarctica and New Zealand (Gibson and Ireland, 1996, Fig. 1). The provenance of the vast volumes of Paleozoic–Mesozoic accretionary sandstone and mudstone sequences incorporated in this margin is an important component for understanding the paleogeography and evolution of the Panthalassan margin. However, in the New Zealand sector of the margin original relative positions have been disrupted by the opening of the Tasman Sea and the Southern Ocean after 80 Ma (Wood, 1994, see also Fig. 1), followed by further disruption and re-configuration of the New Zealand microcontinent up to the present (Sutherland, 1999). Paleogeographic reconstructions of this portion of the margin have therefore been particularly difficult.

2. Basement geology

New Zealand basement geology is described in terms of batholiths, suites and tectonostratigraphic terranes (Bishop et al., 1983; Bradshaw, 1989; Coombs et al., 1976), which are grouped into three provinces: the Western Province, the Median Tectonic Zone (MTZ) and the Eastern Province (Fig. 2). The Western Province comprises two terranes and is largely made up of Lower Paleozoic metasedimentary rocks cut by Devonian, Carboniferous and Early Cretaceous granitoids (Muir et al., 1994, 1997; Waight et al.,

Fig. 1. Present-day distribution of orogenic/mobile belts around the southwest Pacific margin. A = Amundsen Province, R = Ross Province. Insert New Zealand micro-continent indicating the main features discussed in the text. MTZ = Median Tectonic Zone. Adapted from Sutherland (1999).

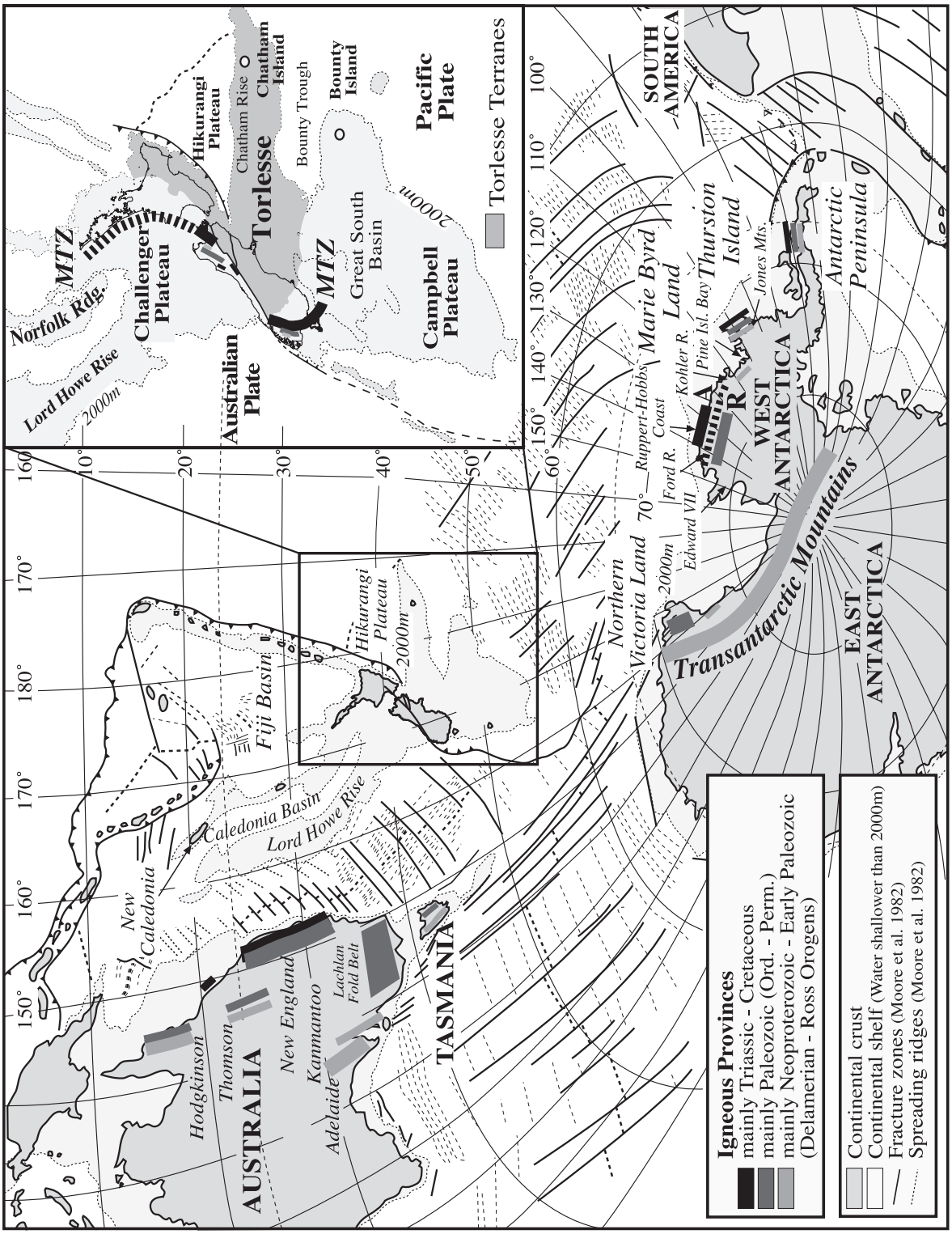
Torlesse Terranes
Hikurangi Plateau
Chatham Island
Chatham Rise
Bounty Trough
Bounty Island
Pacific Plate
MTZ
Challenger Plateau
Torlesse
Great South Basin
Campbell Plateau
Norfolk Rdg.
Lord Howe Rise
2000m
Australian Plate
SOUTH AMERICA
Marie Byrd Land
Thurston Island
Jones Mts.
Antarctic Peninsula
Pine Isl. Bay
Kohler R.
Ruppert-Hobbs Coast
Ford R.
Edward VII
WEST ANTARCTICA
Transantarctic Mountains
EAST ANTARCTICA
Northern Victoria Land
Fiji Basin
Caledonia Basin
New Caledonia
Lord Howe Rise
Hikurangi Plateau
AUSTRALIA
TASMANIA
Hodgkinson
Thomson
New England
Kanmantoo
Lachlan Fold Belt
Adelaide
Igneous Provinces
mainly Triassic - Cretaceous
mainly Paleozoic (Ord. - Perm.)
mainly Neoproterozoic - Early Paleozoic (Delamerian - Ross Orogens)
Continental crust
Continental shelf (Water shallower than 2000m)
Fracture zones (Moore et al. 1982)
Spreading ridges (Moore et al. 1982)

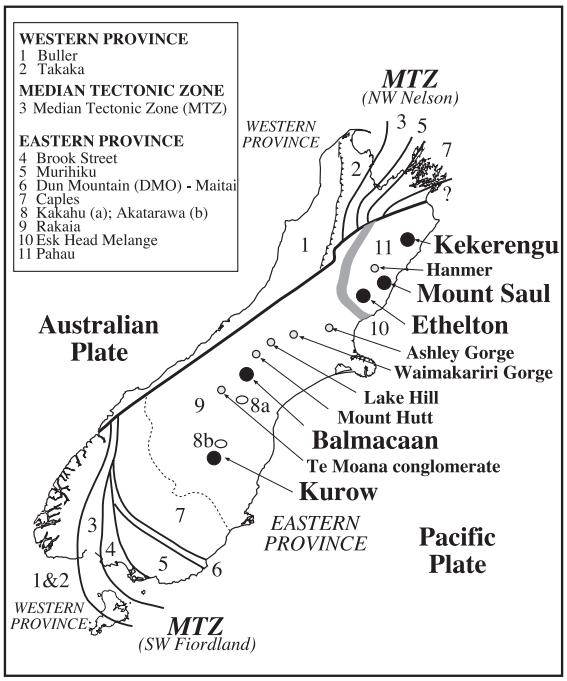

Fig. 2. Tectonostratigraphic terranes map of New Zealand showing distribution of conglomerate locations. Also shown are localities for sandstone samples used for Sr–Nd isotope and U–Pb zircon age (SHRIMP) determination.

1997), with minor volcanic and metamorphic rocks of Cambrian age (Cooper, 1989; Gibson and Ireland, 1996; Münker and Cooper, 1997). It had attained its continental thickness and its gross structure by the end of the Carboniferous and represents a fragment of the Gondwana Paleozoic margin. The Eastern Province consists of arc, forearc and accretionary complex rocks that relate to Permian to Cretaceous plate convergence. The Median Tectonic Zone separates the Western and Eastern Province and consists of suites of Carboniferous to Early Cretaceous subduction-related calc-alkaline plutons with subordinate volcanic and sedimentary rocks (Kimbrough et al., 1994; Mortimer et al., 1999; Muir et al., 1998).

3. Provenance of the Torlesse

The provenance of the Torlesse terranes has occupied New Zealand geologists for many years (Andrews et al., 1976; Bradshaw, 1989; Coombs et al., 1976; Howell, 1980; Korsch and Wellman, 1988; MacKinnon, 1983; Mortimer, 1995; Roser and Korsch, 1999). Sandstone petrography, sedimentary geochemistry, heavy minerals, detrital mineral geochronology and isotope geochemical studies of sediments have all been employed to address this problem (e.g., Adams and Graham, 1996; Cawood et al., 1999; Frost and Coombs, 1989; Ireland, 1992; MacKinnon, 1983; Mortimer, 1995; Pickard et al., 2000; Roser, 1986; Roser and Korsch, 1988, 1999; Smale, 1997). These studies have broadly established a mixed cratonic arc provenance, but on their own are incapable of establishing a specific source. Various sediment sources have been proposed, including a provenance east of present-day New Zealand (Andrews et al., 1976), Marie Byrd Land in Antarctica (Korsch and Wellman, 1988) and the New England Fold Belt in eastern Australia (Adams and Kelley, 1998; Pickard et al., 2000). More local sources have also been proposed for the younger Pahau terrane, such as the older Rakaia terrane (MacKinnon, 1983; Roser and Korsch, 1999; Smale, 1997) or the Median Tectonic Zone (Mortimer, 1995).

Igneous conglomerate clasts are here found to place exceptionally tight constraints on Torlesse provenance and on its Mesozoic tectonic setting within the Southwest Pacific margin of Gondwana. This paper reports provenance data from conglomerates and sandstones in one of the Torlesse terranes, the Pahau terrane. Provenance constraints for the older Rakaia terrane are discussed in a separate paper.

4. Samples and analytical methods

One-hundred and ninety igneous and 24 sandstone clasts were collected from three conglomerates. Criteria for sampling were representation of lithological distribution, degree of alteration, and size (ca. 10 cm). Sandstone petrographic modes were determined by point counting 500 grains in stained thin sections using standard Gazzi-Dickinson method, providing modes considered accurate to within 5% of true values (Van Der Plas and Tobi, 1965). Petrographic procedures and sandstone classification followed MacKinnon (1983). Major and trace element compositions were determined by X-ray fluorescence (XRF) at the University

of Canterbury following Weaver et al. (1990). All elemental concentrations have been renormalised to 100% anhydrous. Rare earth elements (REE) were analysed by instrumental neutron activation (INAA) at the University of Massachusetts, Lowell, using techniques similar to those described by Eby (1984). Selected clasts were submitted for Sr–Nd isotopic analysis and SHRIMP U–Pb zircon dating.

Nd–Sr isotope work was carried out at La Trobe University, Melbourne, following the methods of Waight et al. (1998b). Measured Nd and Sr isotope ratios were normalised to $^{146}Nd/^{144}Nd$= 0.7219 and $^{88}Sr/^{86}Sr$= 8.37521. Average values for the La Jolla Nd and SRM987 Sr standard were 0.511860 ± 15 (2σ) and 0.710230 ± 30 (2σ), respectively. Sr–Nd blanks were < 300 pg and are negligible. Rb/Sr and Sm/Nd ratios for age corrections were derived from XRF and INAA, respectively. Precision for initial $^{87}Sr/^{86}Sr$ is estimated to be ± 0.0001 (2σ) by propagating of errors in Rb/Sr_{XRF} (Rb = 1.995%, Sr = 0.493%, Weaver et al., 1990) and $^{87}Sr/^{86}Sr_{TIMS}$ (± 0.000076 for granitic rock powders and about twice the external precision based on the SRM987 standard). This error covers all possible sources of error including sample powder heterogeneity, but excludes error in the age. A similar calculation for initial εNd (± 10% for Sm and Nd from INAA; ± 0.004% for $^{143}Nd/^{144}Nd_{TIMS}$) produces a combined 2σ error of 0.5 units. In this study, the epsilon notation for Nd (De Paolo and Wasserburg, 1976) is used, which is a measure of the difference between the $^{146}Nd/^{144}Nd$ ratio of a sample or suite of samples and a reference value, which in this case is Chondritic Uniform Reservoir (CHUR).

U–Pb crystallisation ages of igneous clasts and detrital zircons of Rakaia and Pahau sandstones were obtained on SHRIMP RG and SHRIMP I (Sensitive High Resolution Ion Microprobe) at Stanford University in California and at the Australian National University, Canberra. Methods are described in detail by Muir et al. (1997). The ANU standard SL13 was used to normalise the U concentration (238 ppm); the Th concentration was then derived from the Th/U ratio. Duluth standards AS3 and FC1 were used to calibrate U/Pb ratios after correction of Pb^+/U^+ for correlated variation with UO^+/U^+. The Temora standard (417 Ma) was included in one mount as a secondary standard. The zircons are dominated by Phanerozoic material and so emphasis was placed on determining the $^{206}Pb/^{238}U$ age. In order to expedite analysis of the large number of clasts, a relatively small number of analyses (5–10) were performed on each clast. If the data agreed within analytical error, the likelihood is that this represents the igneous age of the clast. If the data were scattered, the likelihood is that many analyses would be required to ascertain the

Table 1
Summary of SHRIMP U–Pb zircon ages for igneous clasts from the three Pahau terrane conglomerates

	Location	UC#	Rock type	Chemistry	Texture	Age	±	MSWD	Comments
L. Jur.–	Kekerengu	30743	biotite	I/S-type	hypidiomorphic	123.1	2.5	0.41	5/6
E. Cret.		30731	rhyolite	I/S-type	strongly porphyritic	134.7	2.0	1.52	6/6
		30738	monzogranite	I/S-type	granophyric	137.5	2.5	1.16	6/6
		30730	rhyolite	I/S-type	porphyritic	142.1	2.2	1.28	5/7 (PbL)
	Ethelton	30964	monzogranite	I/S-type	hypidiomorphic	125.1	2.1	1.18	6/6
		30944	monzogranite	I-type	hypidiomorphic/granophyric	128.2	2.2	0.54	5/6 (Inh)
		30973	rhyolite	I/S-type	strongly porphyritic	136.6	2.1	1.39	5/6 (Inh)
		30952	monzogranite	I/S-type	hypidiomorphic/granophyric	139.0	1.8	0.95	6/6
		30954	rhyolite	I/S-type	strongly porphyritic	140.9	2.0	0.67	5/6 (PbL)
		30925	rhyolite	I/S-type	weakly porphyritic	140.9	2.2	1.09	5/6
	Mount Saul	30823	rhyolite	A-type	weakly porphyritic	141.4	2.9	0.37	6/6
		30867	rhyolite	I/S-type	weakly porphyritic	141.4	2.6	1.14	6/6
		30818	rhyolite	I/S-type	weakly porphyritic	142.4	2.3	0.73	6/6
		30854	rhyolite	A-type	moderately porphyritic	145.2	3.4	0.91	5/6 (Inh)
		30850	monzogranite	I-type	hypidiomorphic/granophyric	146.7	2.9	1.03	5/6 (PbL)
E. Jurassic	Kekerengu	30732	rhyolite	I/S-type	strongly porphyritic	188.3	2.6	0.27	5/6 (Inh)

MSWD = mean square of weighted deviates; 5/6, etc. = proportion of analyses used to calculate mean age (errors are 2 sigma mean and include uncertainty for Pb/U in standard); Inh = inherited component (age>mean); PbL = Pb loss (age < mean).

zircon U–Pb characteristics and even then that result might still be equivocal and further work on these samples was not then undertaken. The uncertainty in the mean, based on 1σ, is of the order of 1.0% for 5 analyses and 0.6% for 10 analyses. After factoring in the uncertainty of the standards, the resultant U–Pb ages are still known at a level of ca. 2%. The zircons from a clast were targeted for the most suitable zircon

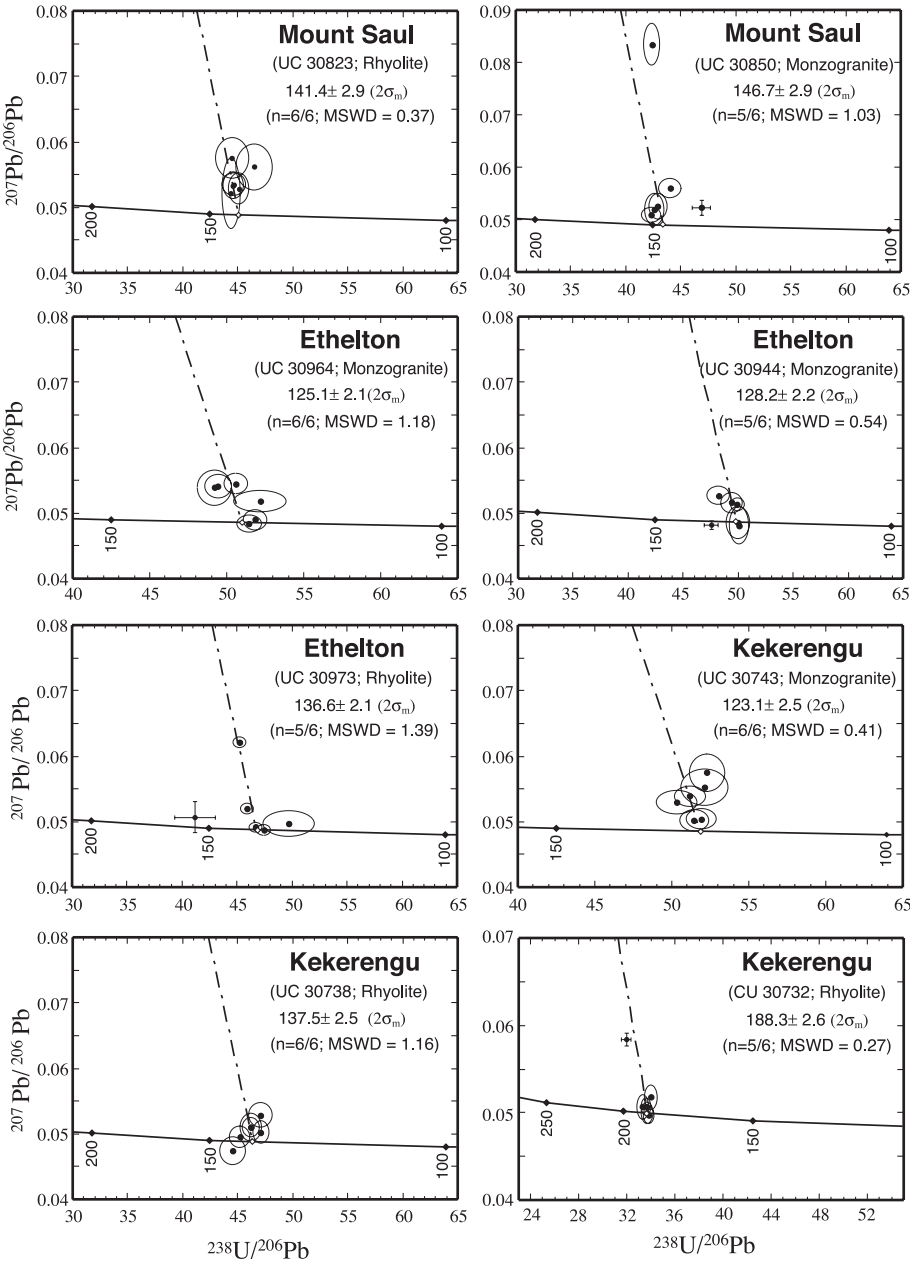

Fig. 3. Selected U–Pb zircon concordia plots (Tera and Wasserburg, 1972) for igneous clasts from the Pahau terrane conglomerate. These plots use the measured Pb isotopic composition (i.e., not corrected for common Pb). The dashed line represents common Pb regression and mean age. The filled dots represent data included in the regression. Error arcs and bars are 1σ.

and spots placed to avoid cracks, inclusions, and other heterogeneities. Cathodoluminescence images were used to optimize spot locations. Detailed descriptions of individual igneous clasts and analysed sandstones are available on request from the authors. The AGSO Phanerozoic Time Scale (Jones, 1995) is used.

Table 2
Chemical analyses of representative igneous clasts from Pahau terrane conglomerates

UC#	Kekerengu					Ethelton						Mount Saul				
	30730	30731	30732	30738	30743	30925	30944	30952	30954	30964	30973	30818	30823	30850	30854	30867
	volc	volc	volc	hypers.	subsol.	volc	subsol.	subsol.	volc	subsol.	volc	volc	volc	subsol.	volc	volc
SiO_2	74.37	70.02	76.44	77.58	73.87	78.38	73.81	76.59	74.64	77.42	73.05	77.30	76.22	70.15	73.32	72.06
Ti_2O	0.22	0.31	0.08	0.15	0.33	0.05	0.26	0.09	0.20	0.09	0.30	0.15	0.27	0.45	0.35	0.35
Al_2O_3	13.58	14.45	12.60	12.49	13.52	12.20	14.24	12.98	13.29	12.41	14.02	12.53	11.83	15.38	13.60	13.98
Fe_2O_3	1.35	3.30	1.25	0.62	1.49	0.52	1.14	0.88	1.88	0.62	2.32	0.77	2.07	2.06	1.93	2.12
MnO	0.03	0.06	0.01	0.01	0.02	0.01	0.04	0.02	0.04	0.02	0.06	0.01	0.09	0.08	0.09	0.09
MgO	0.35	0.58	0.08	0.06	0.25	0.06	0.22	0.14	0.30	0.08	0.54	<0.05	0.10	0.55	0.16	0.31
CaO	0.83	1.12	0.22	0.37	0.59	0.33	1.35	0.71	1.01	0.38	1.32	0.23	0.08	1.32	0.25	0.57
Na_2O	3.86	4.86	4.31	4.55	4.20	3.79	5.16	4.14	4.11	4.23	4.23	4.48	4.28	5.04	5.47	4.23
K_2O	4.35	3.36	4.25	3.72	5.09	4.56	3.08	4.26	3.90	4.25	3.45	4.34	4.67	4.39	4.58	5.30
P_2O_5	0.06	0.07	0.02	0.01	0.06	0.01	0.07	0.01	0.05	0.02	0.09	0.02	0.02	0.13	0.04	0.07
SO_3		2.62	1.25													
LOI	0.98	−0.65	−0.77	0.52	0.22	0.13	0.71	0.29	0.69	0.15	0.97	0.33	0.29	0.45	0.31	0.28
Total	99.98	100.10	99.74	100.08	99.64	100.04	100.08	100.11	100.11	99.67	100.35	100.21	99.92	100.00	100.10	99.36
V	11	22	7	5	22	8	19	10	13	4	30	6	11	21	6	12
Cr	25	10	7	9	12	12	9	7	6	10	17	7	6	9	7	9
Ni	4	6	6	4	7	4	5	3	3	3	3	<3	4	3	4	6
Zn	55	44	17	15	19	26	44	16	30	14	57	23	129	47	88	59
Zr	153	163	138	212	275	88	184	105	136	72	145	410	936	308	597	514
Nb	6	7	11	11	6	9	6	8	6	7	10	13	54	18	24	21
Ba	819	656	553	752	376	256	713	147	643	288	583	77	<20	944	269	392
La	23	27	11	34	35	10	20	9	26	12	34	48	41	38	68	73
Ce	49	56	28	69	65	20	57	27	57	35	58	89	125	69	130	138
Nd	10	19	10	30	21	10	13	10	17	14	23	40	64	43	84	67
Ga	15	16	17	17	16	16	16	16	16	14	17	18	25	17	21	17
Pb	38	23	24	27	19	37	22	26	19	22	22	17	36	16	17	25
Rb	179	132	154	126	387	308	99	162	162	126	145	109	228	148	134	154
Sr	184	220	56	57	86	29	197	44	151	25	169	43	7	241	7	130
Th	18	14	14	13	87	29	7	28	13	10	15	17	20	12	14	19
Y	18	21	21	27	26	16	22	21	21	26	29	40	82	21	56	59
Sc	6	6	3	9	3	4	5	<2	4	5	5	3	5	4	2	8
La													113.3		192.1	205.8
Ce													117.9		152.5	158.4
Nd													76.2		104.8	100.0
Sm													60.6		64.0	62.1
Eu													8.6		27.4	22.6
Gd													42.8		36.6	36.6
Tb													47.0		33.2	34.0
Tm													44.3		26.3	28.0
Yb													40.0		24.1	25.5
Lu													39.7		24.1	25.9
A/CNK	1.08	1.06	1.04	1.02	1.00	1.04	1.00	1.02	1.04	1.01	1.07	1.00	0.97	0.99	0.94	1.02
A/NK	1.23	1.24	1.08	1.08	1.09	1.09	1.20	1.14	1.21	1.07	1.31	1.04	0.98	1.18	0.97	1.10

5. Results

5.1. Conglomerate clast lithology

Conglomerates are rare and constitute < 1% of the Torlesse terranes. Although excellently preserved stratigraphic sections up to a few hundred metres thick are widespread, there is a general lack of marker beds and zones of pervasive tectonic disruption are common. In addition, isoclinal and tight folding is pervasive throughout the Torlesse terrane and stratigraphic control is poor.

The three Pahau conglomerates at Mount Saul, Ethelton and Kekerengu (Fig. 2) are dominated by beds of poorly to moderately sorted, matrix- to clast-supported conglomerates interbedded with massive to thinly bedded, often graded, sandstones. At Ethelton, two distinct conglomerate types are present. One contains a low proportion of matrix of medium to coarse-grained sandstone (15–35% estimated), and includes thin beds of moderately sorted conglomerate interbedded with poorly sorted conglomerate. The other has a higher proportion of matrix (>50% estimated) and is virtually unbedded. Pebbles and boulders in all conglomerates range in size from < 1 to 50 cm and are usually rounded to well rounded, but large angular blocks of sandstones (rip-ups) also occur. Clast populations in all conglomerates are dominated

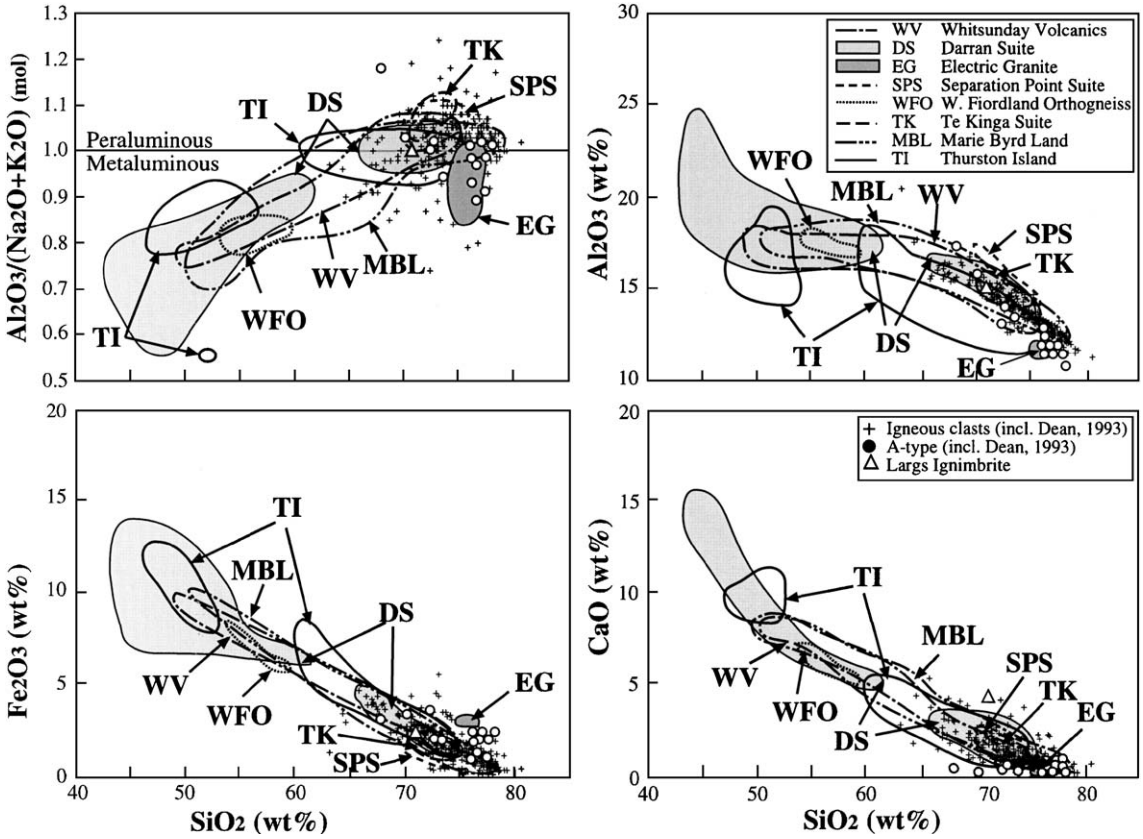

Fig. 4. Major element Harker diagrams for the Late Jurassic to Early Cretaceous Pahau terrane calc-alkaline and peralkaline igneous clasts compared with data from the Median Tectonic Zone in New Zealand, Amundsen Province in Antarctica, and eastern Australia. MTZ includes Darran Suite, Separation Point Suite, Western Fiordland Orthogneiss (Muir et al., 1998). Data for Te Kinga Suite are from Waight et al. (1998b). Amundsen Province includes data from Marie Byrd Land (Ruppert-Hobbs Coast and Pine Island) and Thurston Island. Data for Marie Byrd Land are from (Weaver et al. 1994, and personal communication) and Pankhurst et al. (1993), and those for Thurston Island are from Pankhurst et al. (1993). Eastern Australia data for the Whitsunday Volcanics are from Ewart et al. (1992). Data for the Largs Ignimbrite are from Mortimer (personal communication). Also plotted are data from Dean (1993).

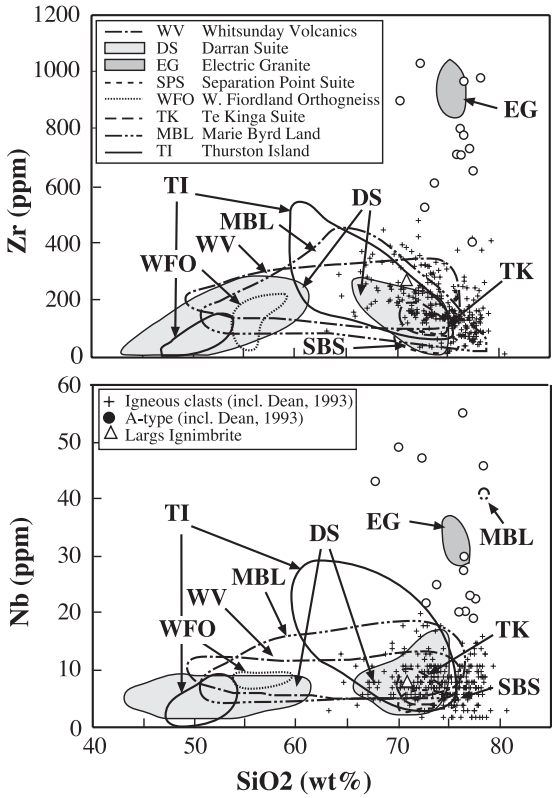

Fig. 5. Trace element Harker diagrams for the Late Jurassic to Early Cretaceous Pahau terrane calc-alkaline and peralkaline igneous clasts compared with data from the Median Tectonic Zone in New Zealand, Amundsen Province in Antarctica, and eastern Australia. MTZ includes Darran Suite, Separation Point Suite, Western Fiordland Orthogneiss (Muir et al., 1998). Data for Te Kinga Suite are from Waight et al. (1998b). Amundsen Province includes data from Marie Byrd Land (Ruppert-Hobbs Coast and Pine Island) and Thurston Island. Data for Marie Byrd Land are from (Weaver et al. 1994, and personal communication) and Pankhurst et al. (1993) and those for Thurston Island are from Pankhurst et al. (1993). Eastern Australia data for the Whitsunday Volcanics are from Ewart et al. (1992). Data for the Largs Ignimbrite are from Mortimer (personal communication). Also plotted are data from Dean (1993).

by sandstones and volcanics. Overall, five lithological groups are distinguished: (1) arenites (Ethelton 60%, Mount Saul 42%, Kekerengu 59%); (2) volcanics (Ethelton 10%, Mount Saul 23%, Kekerengu 10%); (3) lutites (Ethelton 11%, Mount Saul 8%, Kekerengu 18%); (4) granitoids (Ethelton 7%, Mount Saul 13%, Kekerengu 6%); and (5) others including quartz and chert (Ethelton 12%, Mount Saul 14%, Kekerengu 7%).

6. Igneous clasts

6.1. Lithology and petrography

Igneous clasts, both volcanic and plutonic, comprise some 15–35% of clasts in the studied conglomerates. Volcanic clasts are mostly rhyolites, with minor dacites and trachytes. Spherulitic and felsic textures in the matrix of volcanic clasts indicate strong undercooling. However, no pyroclastic clasts were observed and the volcanic clasts are therefore thought to be derived from domes or flows. Rhyolitic clasts from Mount Saul contain riebeckite, a mineral typical of peralkaline igneous rocks. Granitoid clasts are mostly monzogranite and leucomonzogranite; granodiorites and leucosyenogranites are less common. Hypersolvus

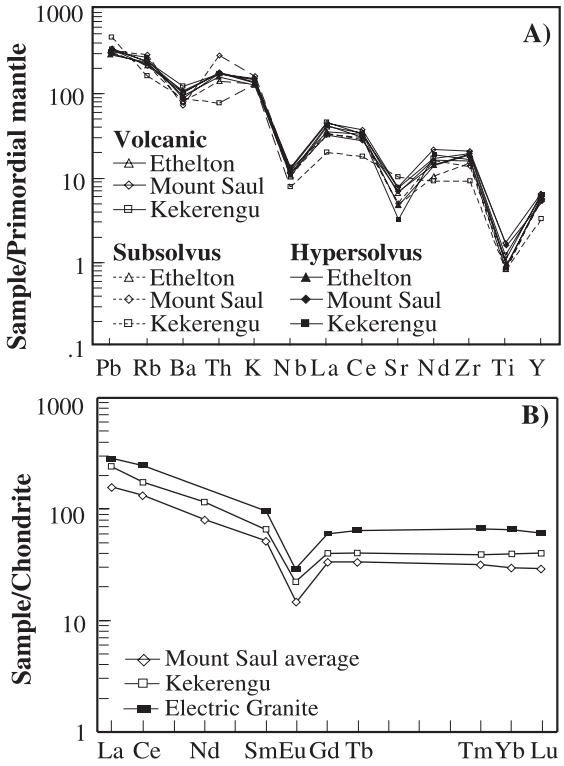

Fig. 6. (A) Mantle normalised (McDonough et al., 1992) multi-element diagram. Averages of all the selected subsolvus, hypersolvus and igneous clasts from the three Pahau terrane conglomerates. (B) Chondrite normalised (Nakamura, 1974) average REE content of the Mount Saul (averaged) and Kekerengu alkaline samples and Electric Granite (Muir et al., 1998) of the Median Tectonic Zone.

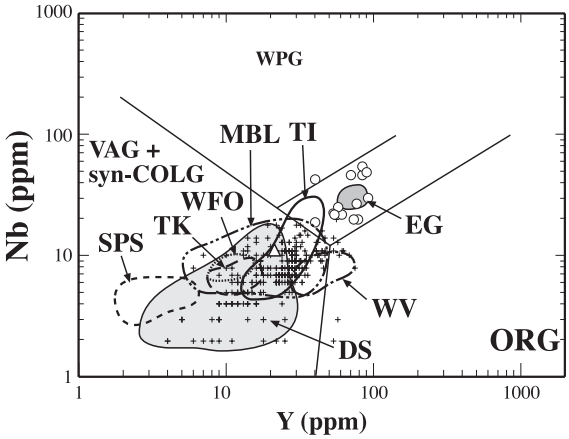

Fig. 7. Tectonic discrimination diagram after Pearce et al. (1984) comparing igneous conglomerate clasts with igneous provinces from the SW Pacific margin. Fields are for syn-collision-granite (syn-COLG), volcanic-arc-granite (VAG), within-plate-granite (WPG) and ocean-ridge-granite (ORG).

clasts are distinctly granophyric and can easily be distinguished from subsolvus clasts, which are generally undeformed.

Metamorphism in the studied Torlesse conglomerates is low grade and the conglomerates are largely non-schistose. Chlorite commonly replaces mafic silicates (mostly biotite, but also hornblende and clinopyroxene). Epidote is associated with and replaces plagioclase and is sometimes accompanied by calcite. Granular titanite often accompanies chlorite and epidote and also occurs marginally to opaque oxide mineral grains. All our sample locations are within the zeolite facies and much of the observed alteration is thus metamorphic in origin.

6.2. U–Pb zircon ages

SHRIMP U–Pb data for 16 igneous clasts are summarised in Table 1 and shown on Tera and

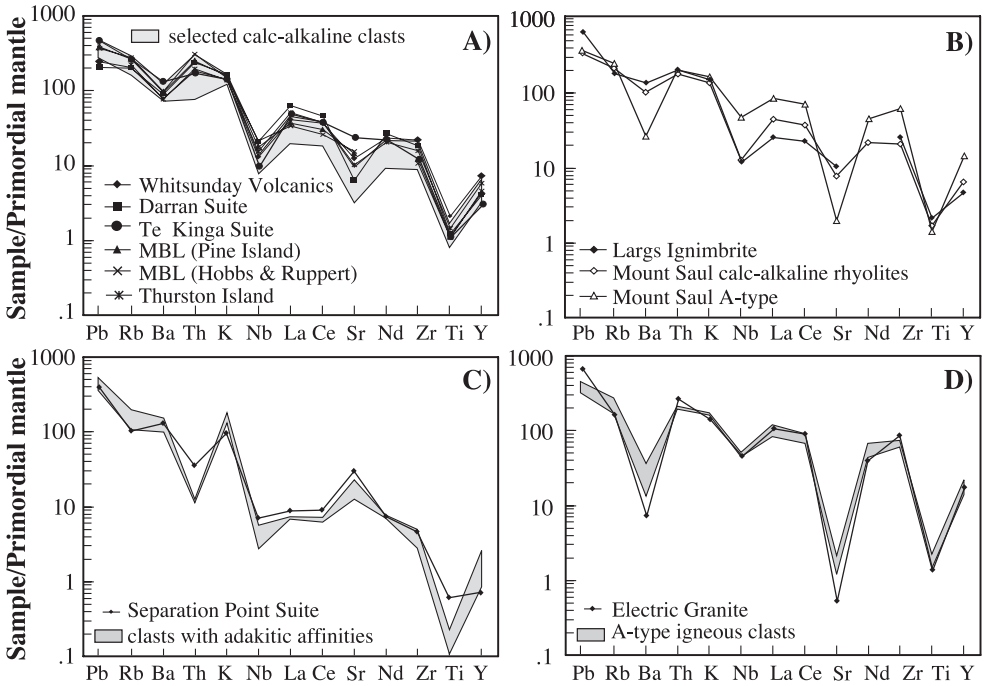

Fig. 8. Mantle normalised (McDonough et al., 1992) multi-element diagrams. (A) Averages of selected calc-alkaline igneous clasts from the three Pahau terrane conglomerates are compared with selected granitoids and volcanics from igneous provinces from the SW Pacific. (B) Volcanic calc-alkaline igneous clasts are compared with alkaline clast from Mount Saul and the Largs Ignimbrite. (C) Adakitic clasts are compared with Separation Point Suite rocks from the Median Tectonic Zone. (D) Alkaline clasts are compared with the Electric Granite from the Median Tectonic Zone.

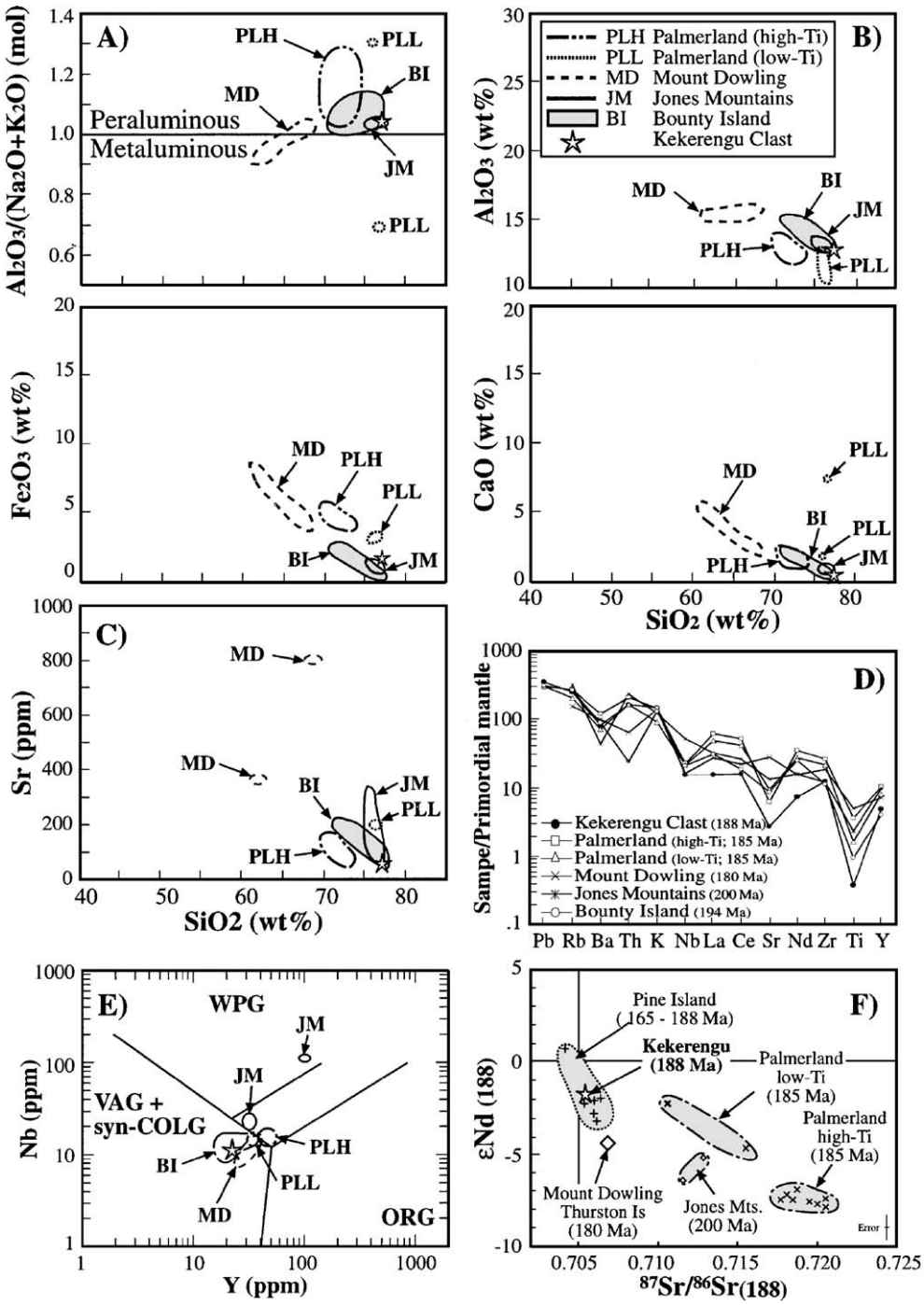

Fig. 9. Major and trace element Harker diagrams (A to C), mantle normalised (McDonough et al., 1992) multi-element diagram (D), tectonic discrimination diagram (E) and $\varepsilon Nd_{(188)}$ versus $^{87}Sr/^{86}Sr_{(188)}$ diagram (F) for the Early Jurassic igneous clast from Kekerengu compared with selected Lower to early Middle Jurassic source rocks from Palmerland (Mount Poster Fm, Riley et al., 2001), Jones Mountains (Eights Coast), Mount Dowling (Thurston Island) and Pine Island (Pankhurst et al., 1993, Pankhurst, unpublished data), and Bounty Island (Dean, 1993). Error bars represent ± 0.5 εNd and 0.0001 for Sr isotopes.

Wasserburg (1972) diagrams in Fig. 3. The majority of ages are upper Late Jurassic to Early Cretaceous (147–123 Ma), but one Kekerengu clast gave an Early Jurassic age (188 ± 3 Ma). The 147–123-Ma age range for the majority of clasts is similar to the periods of granite magmatism in the MTZ and the Western Province.

6.3. Chemistry and Sr–Nd isotopes

Two major geochemical groups have been identified within the igneous clast population: (1) a calc-alkaline group and (2) a peralkaline group. A third, minor group consists of a few clasts from Kekerengu which have adakitic affinities. Representative analyses are listed in Table 2 and selected geochemical plots are presented in Figs. 4–8. The single Early Jurassic clast from Kekerengu is chemically very similar to the calc-alkaline group but is plotted separately in Fig. 9. The calc-alkaline clasts vary widely in composition, with SiO_2 from 63 to 81 wt.%, but most samples have 74–78% SiO_2. Most plot near the felsic end of a typical calc-alkaline to high-K calc-alkaline series of Peccerillo and Taylor (1976). Weakly peraluminous clasts dominate over metaluminous clasts but only a few peraluminous samples were found (Fig. 4). A cogenetic relationship between the calc-alkaline clasts from all three conglomerates (granitic and volcanic) is indicated by coherent major and trace element trends (Figs. 4 and 5) and by near identical multi-element trends (Fig. 6A). Clasts with peralkaline affinities are typically enriched in Zr and Nb (Fig. 5) and have REE characteristics typical of A-type granites (Eby, 1990, Fig. 6B). Nb–Y systematics (Fig. 7) suggest the peralkaline clasts have within-plate signatures whereas most of the calc-alkaline clasts show predominantly volcanic-arc signatures (Pearce et al., 1984).

Sr–Nd isotope results are listed in Table 3. Initial Sr isotope ratios ($^{87}Sr/^{86}Sr_i$) range from 0.7026 to 0.7062; the results for two of the peralkaline Mount Saul clasts are < 0.700 and are thus clearly unrealistic. Both samples have < 10 ppm Sr and very high Rb/Sr and are therefore very sensitive to even minor errors in age corrections and/or to alteration. Initial εNd (εNd_i) ranges from +3.9 to −1.9 and shows an overall negative correlation with $^{87}Sr/^{86}Sr_i$. Mount

Table 3
Sr–Nd isotope data for igneous clasts from the three Pahau terrane conglomerates

	UC#	Type	Age (Ga)	Rb (ppm)	Sr (ppm)	$^{87}Rb/^{86}Sr$	$^{87}Sr/^{86}Sr_{(m)}$	$^{87}Sr/^{86}Sr_{(i)}$	Sm (ppm)	Nd (ppm)	$^{147}Sm/^{144}Nd$	$^{143}/^{144}Nd_{(m)}$	$\varepsilon Nd_{(0)}$	$\varepsilon Nd_{(i)}$	T_{DM}
Kekerengu	30743	monzogranite	0.123	387	86	13.06	0.72619	0.70336	5.49	30.73	0.1080	0.512722	1.6	3.0	0.6
	30731	rhyolite	0.135	130	215	1.75	0.70927	0.70592	3.83	20.97	0.1105	0.512566	−1.4	0.1	0.9
	30738	monzogranite	0.138	133	57	6.72	0.71879	0.70560	6.14	31.88	0.1165	0.512537	−2.0	−0.6	1.0
	30730	rhyolite	0.142	179	184	2.82	0.71108	0.70540	2.96	16.56	0.1079	0.512566	−1.4	0.2	0.8
	30732	rhyolite	0.188	154	55	8.05	0.72713	0.70560	2.54	10.32	0.1486	0.512482	−3.0	−1.9	1.6
Ethelton	30964	monzogranite	0.125	131	25	15.53	0.73195	0.70436	3.38	14.78	0.1382	0.512657	0.4	1.3	1.0
	30944	monzogranite	0.128	102	198	1.49	0.70877	0.70606	4.06	22.41	0.1094	0.512590	−0.9	0.5	0.8
	30973	rhyolite	0.137	148	171	2.49	0.71108	0.70622	5.37	25.64	0.1265	0.512486	−3.0	−1.7	1.2
	30952	monzogranite	0.139	165	45	10.67	0.72565	0.70457	1.96	9.46	0.1250	0.512578	−1.2	0.1	1.0
	30954	rhyolite	0.141	164	152	3.13	0.71191	0.70564	3.83	20.26	0.1143	0.512566	−1.4	0.1	0.9
	30925	rhyolite	0.141	306	29	30.47	0.76498	0.70390	2.19	6.62	0.1997	0.512575	−1.2	−1.3	6.2
Mount Saul	30823	rhyolite	0.141	222	7	94.57	0.88587	0.69634	11.55	45.91	0.1521	0.512768	2.5	3.3	1.0
	30867	rhyolite	0.141	153	130	3.42	0.71065	0.70379	11.49	61.09	0.1137	0.512703	1.3	2.8	0.7
	30818	rhyolite	0.142	114	43	7.68	0.71814	0.70264	5.94	31.69	0.1134	0.512759	2.4	3.9	0.6
	30854	rhyolite	0.145	130	7	57.51	0.81791	0.69938	11.81	62.26	0.1146	0.512682	0.9	2.4	0.7
	30850	monzogranite	0.147	146	238	1.78	0.70771	0.70398	4.70	28.03	0.1015	0.512693	1.1	2.9	0.6

Maximum propagated errors (2S.D.) are ± 0.0001 for $^{87}Sr/^{86}Sr_i$ and ± 0.5 units for εNd_i.

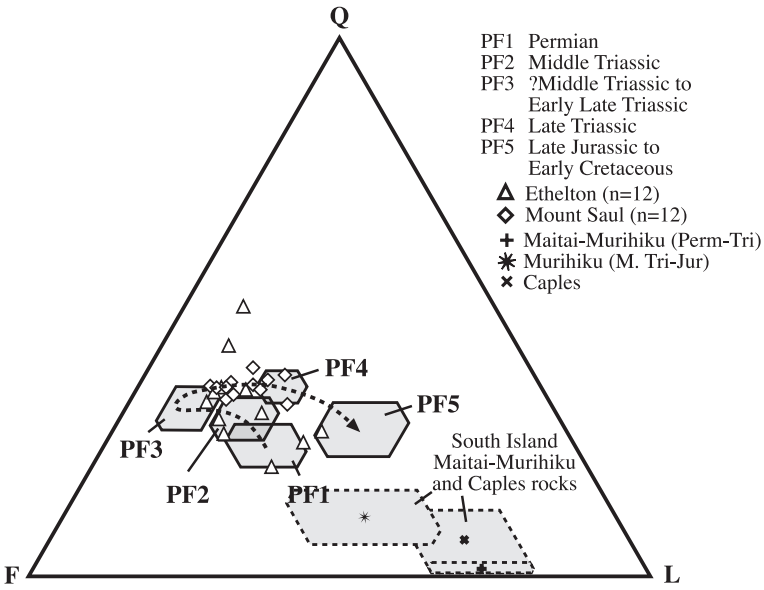

Fig. 10. Q–F–L diagram for sandstone clasts from the Ethelton and Mount Saul conglomerates compared with Rakaia sandstones. Hexagons for the five Torlesse sandstone petrofacies (PF1–5) are one standard deviation about the mean according to MacKinnon (1980). Arrow shows the evolution trend of the Torlesse sandstone.

Saul igneous clasts have the most primitive Sr–Nd isotopic compositions (0.70264–0.70398, +3.9 to +2.8), while Ethelton (0.7039–0.7062) and Kekerengu (0.7033–0.7059) clasts show similar Sr isotopic ranges. Kekerengu clasts show the widest range in εNd_i (+1.6 to −3.0), bridging the gap between the

Table 4
Composition of sandstone clasts from the Ethelton and Mount Saul conglomerates

# Samples	Ethelton 12				Mount Saul 12			
Location	Min	Max	Mean	S.D.	Min	Max	Mean	S.D.
Size	0.20	0.40	0.28		0.25	0.45	0.32	
Quartz	14	40	22		24	28	26	
Polyquartz + chert	1	6	3		1	4	2	
Potassium feldspar	4	17	10		10	18	14	
Plagioclase	22	35	29		22	29	25	
Volcanic lithics	6	22	11		7	16	10	
Metamorphic lithics	0	2	1		1	2	1	
Sedimentary lithics	0	6	3		1	6	3	
Mica	2	7	5		3	8	6	
Heavy minerals	1	6	4		3	7	5	
Others (cement + alterite)	1	1	1		0	1	1	
Matrix	5	14	11		4	9	7	
Q			31.7	8.1			34.6	1.9
F			48.9	5.7			48.0	4.3
L			19.4	8.5			17.4	4.1
P/F			0.75	0.09			0.64	0.05
Lv/L			0.71	0.12			0.70	0.05
%M			5.90	1.90			6.50	1.90

Q = framework quartz, F = feldspar, L = lithic fragments; contents have been recalculated to 100%; P/F = plagioclase to total feldspar ratio; Lv/L = volcanic lithic fragment to total lithic fragment ratio; %M = framework percent mica. Alterites are detrital framework grains altered beyond recognition. Point counts were of a minimum of 500 grains. Procedures, definitions of parameters, and grain types follow MacKinnon (1980).

isotopically primitive Mount Saul clasts and the more evolved Ethelton clasts (− 1.7 to + 1.3).

7. Sedimentary clasts and sediments

Sandstone clasts (arenites) comprise 42–60% of the Pahau conglomerate clast populations. Earlier workers suggested derivation of these clasts from older Torlesse units (Barnes, 1990; MacKinnon, 1983; Smale, 1978). Our study of sandstone clasts from Ethelton and Mount Saul provides the first unequivocal petrographic and geochemical evidence for such a recycling. Salient points are given below; for a more comprehensive discussion, see Wandres et al. (submitted to NZJGG.)

7.1. Petrography

The sandstone clasts from Ethelton and Mount Saul are immature, moderately sorted, angular feldspathic arenites with a restricted range of Q–F–L compositions averaging $Q_{30}F_{49}L_{21}$ (Fig. 10). Petrographic modes for clasts from the two localities overlap, but the Ethelton clasts tend to have lower framework %quartz and %mica mean content, higher lithics, and plagioclase and total feldspar framework ratios, and a slightly higher volcanic lithics to total lithics framework ratio (Table 4).

MacKinnon (1983) established five petrofacies (PF) that correspond approximately to ages based on sparse fossil control (Campbell and Warren, 1965;

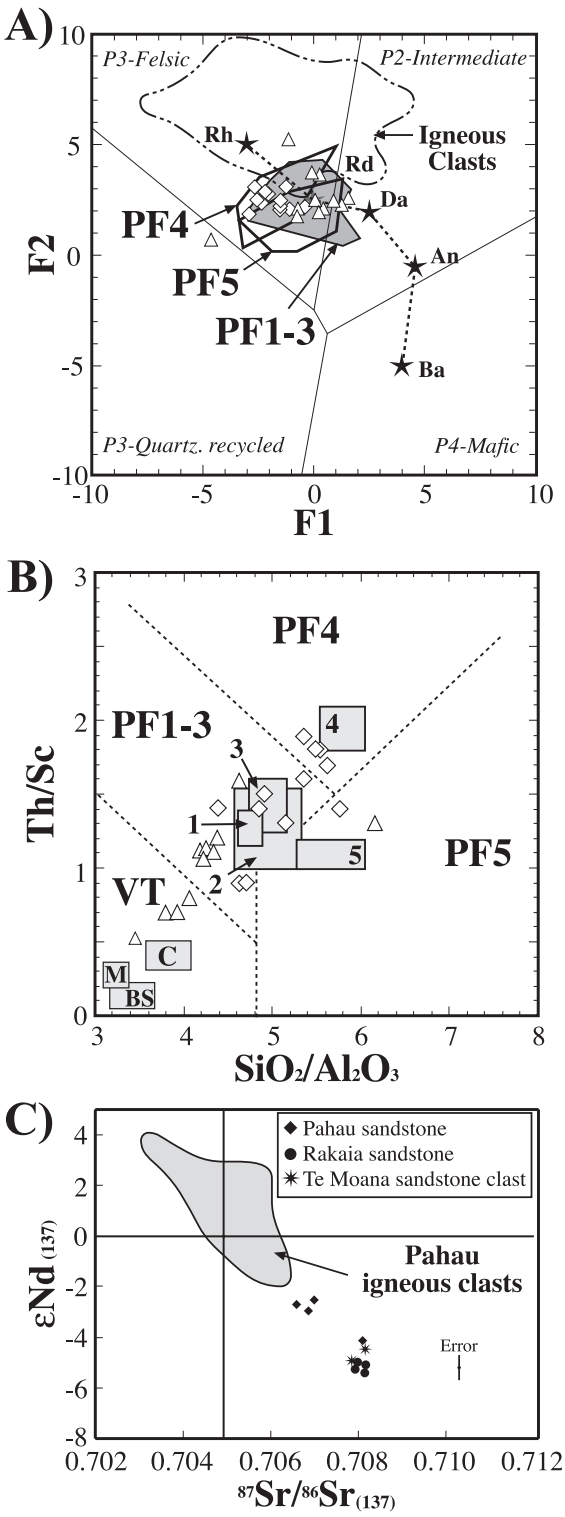

Fig. 11. Chemistry for sandstone clasts from the Ethelton and Mount Saul conglomerates compared with Rakaia sandstones. (A) Discriminant function plot (Roser and Korsch, 1988). Fields P1–P5 and igneous averages Ba = basalt, An = andesite, Da = dacite, Rd = rhyodacite and Rh = rhyolite are from Roser and Korsch (1988) and Roser and Korsch (1999). $F1 = -1.773TiO_2 + 0.607Al_2O_3 + 0.76FeO_t - 1.5MgO + 0.616CaO + 0.509Na_{a2}O - 1.224K_2O - 9.09$; $F2 = 0.445TiO_2 + 0.07Al_2O_3 - 0.25FeO_t - 1.142MgO + 0.438CaO + 1.475Na_2O + 1.426K_2O - 6.861$. (B) $Th/Sc - SiO_2/Al_2O_3$ diagram. Petrofacies fields are from Roser and Korsch (1999). VT = volcanogenic terrane field, C = Caples Trn, BS = Brook Street Trn, M = Maitai Trn. The boxes are 95% confidence fields and the numbers 1–5 = Tolesse petrofacies. (C) $\varepsilon Nd_{(137)}$ versus $^{87}Sr/^{86}Sr_{(137)}$ for Pahau igneous clasts compared with Pahau and Rakaia terrane sandstones and sandstone clasts from the Te Moana conglomerate. Error bars represent ± 0.5 εNd and 0.0001 for Sr.

Speden, 1974). PF1–4 are confined to the Rakaia terrane (Permian to Triassic) and PF5 corresponds to the Pahau terrane. The clast modes plot across the Rakaia PF1–4 petrofacies fields; only one plots marginally in the Pahau PF5 field.

7.2. Geochemistry

On a discriminant function plot (Roser and Korsch, 1988) most of the sandstone clasts plot close to average rhyodacite composition (Rd, Fig. 11A) and are indistinguishable from Rakaia PF1–PF3 sandstones. Almost none of the samples plot in the area in which only Pahau sandstones (PF5) fall, confirming petrographic identification of the clasts as Rakaia (Fig. 11A). In a SiO_2/Al_2O_3–Th/Sc diagram (Fig. 11B), the Mount Saul sandstone clasts plot across all the Torlesse petrofacies fields and are the only clasts that extend into PF4. Clasts from Ethelton generally plot within the PF1–3 field but extend into the volcanogenic field.

7.3. Sr–Nd isotopes

Isotopic data for two sandstone clasts and eight sandstones are presented in Table 5. Four of the sandstones are from the Pahau terrane (including one each from Mount Saul and from Ethelton), another four are from the Rakaia terrane (three from PF4, one from PF3). In addition, two sandstone clasts from the Te Moana conglomerate in the Rakaia terrane were also studied. The latter are considered to be cannibalistically recycled Rakaia material (see previous section) and are probably of Permian age.

For comparison with the igneous Pahau conglomerate clasts (Fig. 11C), the sandstone isotopic results were age-corrected to a common age of 137 Ma. This is the mean age of all igneous clasts (excluding the Early Jurassic clast) and broadly coincides with an older depositional age of the Pahau sandstone. The Pahau sandstones from Mount Saul and Hanmer Basin have similar isotope ratios (0.7066–0.7070; +2.6 to −2.9) but differ from the Ethelton sandstone sample (0.7081, −4.1). The latter shows affinities with the Rakaia sandstones and sandstone clasts (0.7078–0.7082, −4.4 to −5.5). Despite the distortion of original isotope relationships by the

Table 5
Sr–Nd isotope and selected trace element data for sandstone clasts from the Permian Te Moana conglomerate and for sandstones from the Rakaia and Pahau terranes

	Terrane	UC#	Location	Age (Ma)	Rb (ppm)	Sr (ppm)	$^{87}Rb/^{86}Sr$	$^{87}Sr/^{86}Sr_{(m)}$	$^{87}Sr/^{86}Sr_{(i)}$	Sm (ppm)	Nd (ppm)	$^{147}Sm/^{144}Nd$	$^{143/144}Nd$	$\varepsilon Nd^{1}_{(0)}$	$\varepsilon Nd^{2}_{(i)}$	T_{DM}	Th	Sc	Th/Sc
Sandstone clasts	Rakaia	32231	Te Moana	260	91	380	0.691	0.70951	0.70696	5.10	27.65	0.112	0.51233	−5.1	−3.1	1.2	13	10	1.3
		32232	Te Moana	260	48	371	0.372	0.70856	0.70718	5.01	27.81	0.109	0.512310	−6.4	−3.5	1.2	11	11	1.0
Sandstones	Rakaia	32283	Lake Coleridge	230	80	427	0.545	0.70922	0.70744	4.27	23.58	0.109	0.512297	−6.7	−4.1	1.3	10	9	1.1
		32284	Hutt Creek	230	60	547	0.318	0.70857	0.70753	4.57	26.27	0.105	0.512288	−6.8	−4.1	1.2	10	9	1.1
		32286	Waimakariri Gorge	230	39	488	0.229	0.70859	0.70787	4.32	23.25	0.112	0.512285	−6.9	−4.5	1.3	8	8	0.9
	Pahau	32288	Ashly Gorge	230	86	513	0.488	0.70894	0.70741	5.95	31.66	0.113	0.512307	−6.5	−4.1	1.3	13	12	1.1
		32281	Ethelton	115	84	175	1.396	0.71084	0.70856	3.90	20.84	0.113	0.512353	−5.6	−4.3	1.2	7	12	0.6
		31598	Hanmer	120	70	279	0.731	0.70804	0.70679	4.10	21.29	0.116	0.512429	−4.1	−2.8	1.1	7	12	0.6
		31604	Hanmer	120	80	266	0.870	0.70854	0.70706	4.02	21.83	0.111	0.512414	−4.4	−3.1	1.1	8	14	0.6
		32262	Mount Saul	120	89	249	1.036	0.70900	0.70723	3.74	19.91	0.114	0.512435	−4.0	−2.7	1.1	7	13	0.5

Maximum propagated errors (2S.D.) are ±0.0001 for $^{87}Sr/^{86}Sr_i$ and ±0.5 units for εNd_i.

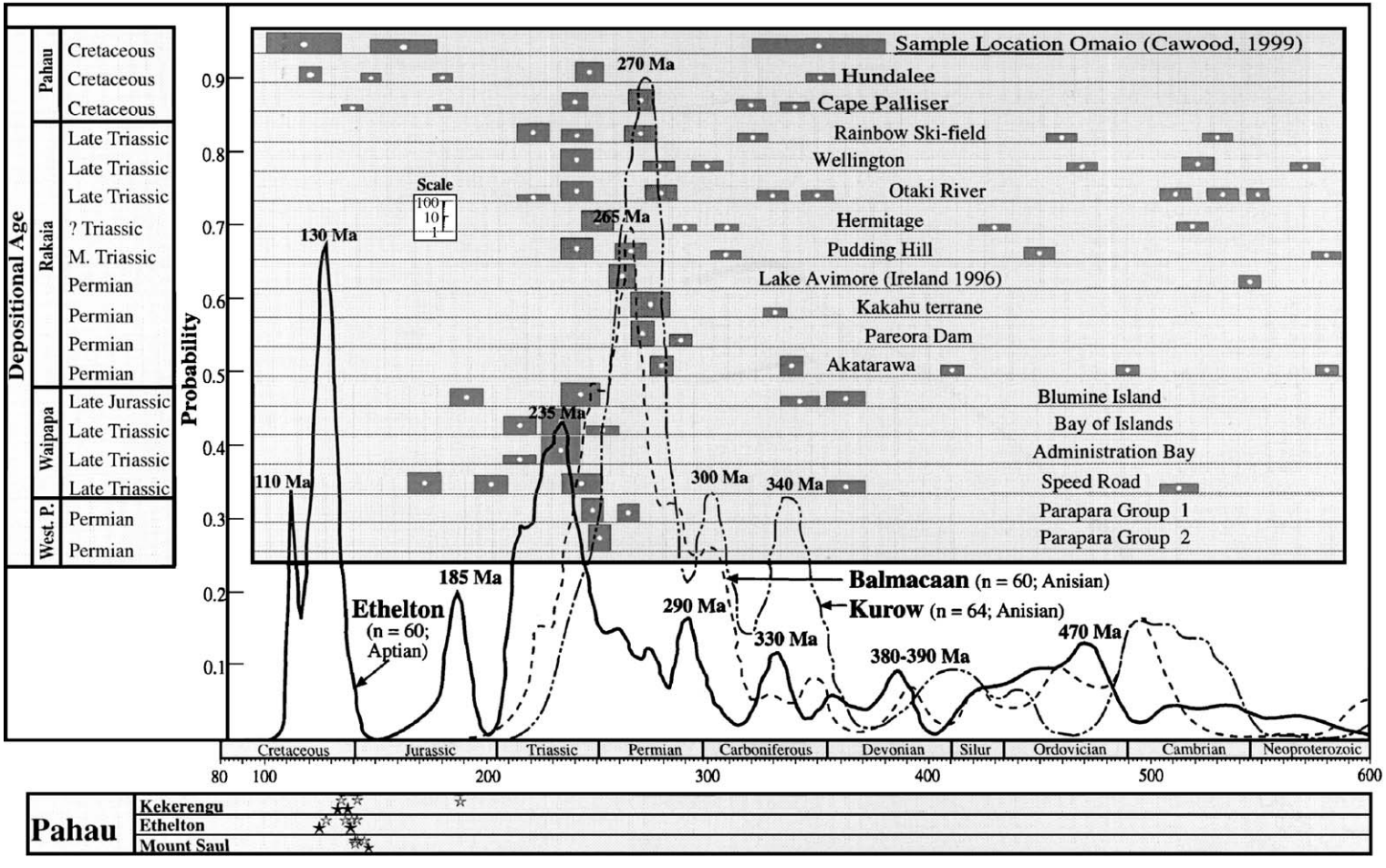

Fig. 12. Cumulative probability distribution curves of zircon ages for the Ethelton conglomerate matrix and the two Rakaia terrane sandstones from Kurow and Balmacaan. Detrital zircon age data from Cawood et al. (1999), Ireland (1992), Pickard et al. (2000) and Wysoczanski et al. (1997) are plotted in the grey shaded box. The dots represent the peaks from cumulative probability curves and the boxes represent, on the horizontal axis, the age range of the major and minor groups, and on the vertical axes, the proportion of these components (as % on a logarithmic scale). Igneous clast ages from the Pahau conglomerates are plotted on the lower bar for comparison. Diagram adapted from Pickard et al. (2000).

common age correction to 137 Ma, εNd_i values are not greatly affected and clearly distinguish the provenance of the sandstones from that of the igneous clasts.

7.4. Detrital U–Pb zircon ages

Zircon U–Pb ages for two Rakaia terrane sandstones (Kurow, Balmacaan localities, Fig. 2) and for a matrix sample of the Ethelton conglomerate were obtained to investigate if recycling of older Torlesse sediments can be demonstrated. Zircon age distribution patterns shown as cumulative probability curves in Fig. 12 are compared with the patterns for sandstones from the Caples, Rakaia and Pahau terranes, and for sandstones from the western Province (Cawood et al., 1999; Ireland, 1992; Pickard et al., 2000; Wysoczanski et al., 1997).

The two Rakaia terrane sandstones contain a major age group in the range 360–220 Ma (Devonian–Middle Triassic), comprising 51% and 70% of the respective data sets. The major peak in the Permian Kurow sample (ca. 270 Ma) is indistinguishable from that in other Permian Rakaia sandstones (Fig. 12). The pattern for the Middle Triassic (Anisian) Balmacaan Stream sandstone agrees well with that of another Middle Triassic sandstone collected nearby (Pudding Hill, PUD1, Pickard et al., 2000), but has a slightly older main peak at 265 Ma.

The major age group in the Lower Cretaceous (Aptian) Ethelton matrix sample (240–200 Ma, 25% of ages) is indistinguishable from the major age group recognised in various Triassic Rakaia, Waipapa/Caples, and Western Province sandstones. The peak at ca. 235 Ma coincides exactly with peaks reported in these sandstones. Other age peaks in the Ethelton conglomerate matrix (at 130, 180 and 330 Ma) are also found in sandstones from other Pahau localities.

8. Discussion

8.1. Mesozoic igneous provinces of the SW pacific

Igneous provinces of the now dispersed Gondwana margin (Fig. 1) are briefly described in order to compare and correlate their petrography, geochemistry and geochronology with those of the Early Jurassic to Early Cretaceous Pahau igneous clasts. Only igneous suites and plutons with ages and geochemical–isotopic compositions similar to those of the igneous clasts are considered.

From the Jurassic to Early Cretaceous, the SW Pacific margin of Gondwana was dominated by oblique subduction (Bradshaw, 1989; Luyendyk, 1995), large-scale strike-slip faulting (DiVenere et al., 1995), diachronous magmatic events, and significant compositional variation in magma production. Calc-alkaline magmatism, related to subduction, is characteristic of terranes recognised in New Zealand (MTZ, Kimbrough et al., 1994; Muir et al., 1994; Muir et al., 1998) and Antarctica (Amundsen Province, Pankhurst et al., 1993; Pankhurst et al., 1998; Weaver et al., 1994). In both areas, a rapid change to extensional tectonics in the mid-Cretaceous (e.g., formation of metamorphic core complexes, Gibson et al., 1989; Luyendyk et al., 1996; Spell et al., 2000; Tulloch and Kimbrough, 1989) was followed by rifting of the Campbell Plateau from Marie Byrd Land, and of the Western Province from Australia.

8.1.1. Eastern Australia

The Whitsunday Volcanic Province extends along the central and southern Queensland coast (Bryan et al., 2000; Ewart et al., 1992). Volcanic and intrusive activity occurred from 132 to 95 Ma, with a major volcanic episode between ca. 120 and 105 Ma (Bryan et al., 1997; Ewart et al., 1992). K/Ar data from the western Whitsunday Volcanic Province suggests early magmatism at 145 Ma (Allen et al., 1998). An extension of the Whitsunday Volcanic Province into New Zealand prior to Gondwana break-up has been suggested (Bryan et al., 2000; Ewart et al., 1992).

8.1.2. New Zealand

8.1.2.1. Median tectonic zone. Most calc-alkaline plutonic rocks of the MTZ south of the Alpine Fault (SW Fiordland) range in age from 168 to 137 Ma and were placed into the bimodal (gabbro-diorite, granodiorite–monzogranite) Darran Suite (Muir et al., 1998). The Darran Suite is intruded by Early Cretaceous adakitic Separation Point-type granites (ca. 124 Ma) which are slightly older than the Separation Point Batholith in NW Nelson (117 ± 2

Ma, Muir et al., 1997) but similar in age to the Western Fiordland Orthogneiss of Fiordland. The Electric Granite (137 ± 2 Ma) is distinctly peralkaline. The metaluminous Largs Ignimbrite (140 ± 2 Ma, Mortimer et al., 1999), tentatively correlated with the Glade Suite in the Darran Complex, suggests that Late Jurassic–Early Cretaceous plutonism in the MTZ was accompanied by volcanism. Evidence of widespread mafic Late Jurassic to Early Cretaceous volcanism within the MTZ is indicated by the Palisade and Big Bush Andesites, the Drumduan Group, Rainy River conglomerate and the Patterson Group (Johnston et al., 1987; Kimbrough et al., 1994; Tulloch et al., 1999).

8.1.2.2. Bounty Island. Weakly peraluminous calc-alkaline granites (Tulloch, 1983) have given a SHRIMP U–Pb zircon age of 194 ± 5 Ma (Ireland, personal communication). Cook et al. (1999) placed the Bounty Island Granite tentatively within the Median Tectonic Zone.

8.1.2.3. Buller terrane. The Crow Granite (137 ± 3 Ma) is similar in age and geochemistry to plutons from the MTZ (Muir et al., 1997). Waight et al. (1998b) recognised two distinct but related suites (Te Kinga and Deutgam) in the Hohonu Batholith, with the bulk of the plutons emplaced in the mid-Cretaceous (114 to 109 Ma). The relatively mafic, metaluminous, I-type Deutgam Suite and the peraluminous, high silica Te Kinga Suite are characterised by restricted radiogenic isotopic compositions. The Te Kinga Suite is weakly adakitic and similar in chemistry to the Separation Point Suite. The tholeiitic Kirwans dolerites (172–151 Ma), correlative with the Ferrar magmatic province (Mortimer et al., 1995), are the only Early Jurassic intrusions within the Buller terrane. However, their distinct tholeiitic geochemistry and highly radiogenic isotope composition make these rocks an unlikely source for the Pahau Early Jurassic igneous clast population.

8.1.3. Antarctica

8.1.3.1. Marie Byrd Land. Weaver et al. (1994) described a mid-Cretaceous (124–108 Ma) calc-alkalic, metaluminous suite from the Ruppert-Hobbs Coast, ranging in composition from diorite to monzogranite. In Pine Island Bay, granitoids range in age from 125 to 114 Ma but have a slightly more primitive isotopic composition compared with Ruppert-Hobbs (Weaver et al., 1996; Pankhurst, personal communication). Granodiorites from the Kohler Range and Pine Island Bay yield ages between 105 and 95 Ma and so are too young to be considered as a clast source. Unpublished Sr/Nd isotope data (Pankhurst, personal communication) from Pine Island Bay indicate that six samples are of Early to Middle Jurassic age (ca. 178 Ma).

8.1.3.2. Thurston Island. Pankhurst et al. (1993) and Leat et al. (1993) recognised two major periods of magmatism on Thurston Island and the adjacent Eights Coast, one in the Late Jurassic (152–142 Ma) and the second in the Early Cretaceous (125–110 Ma). Compositions range from gabbro to felsic granites but form a uniformly calc-alkaline, predominantly metaluminous suite (Leat et al., 1993). Early Jurassic (ca. 200 Ma) granitoids have been reported from the Jones Mountains, and volcanic and volcanogenic rocks from Mount Dowling (ca. 180 Ma) in central Thurston Island (Mukasa and Dalziel, 2000; Pankhurst et al., 1993).

8.1.3.3. Antarctic Peninsula. Early–Middle Jurassic magmatism was reviewed by Pankhurst et al. (2000) and Riley et al. (2001, their Fig. 1), who recognised three distinct magmatic episodes (V1, 188–178 Ma; V2, 172–162 Ma; V3, 157–153 Ma). V1 and V2 are confined to the Antarctic Peninsula (Palmerland) and possibly Thurston Island (Pankhurst et al., 2000, their Fig. 10). Only the V1 rhyolites are considered here as a potential source for early Jurassic Pahau igneous clasts because the other granitoids are the wrong age or have unsuitable Sr–Nd isotope ratios (Millar et al., 2001). Based on a Jurassic pre-break-up configuration of the Gondwana margin (e.g., Riley et al., 2001), Middle-Jurassic (ca. 175 Ma) peraluminous granitoids within the Ellsworth-Whitmore Mountains (Storey et al., 1988) are here considered too distal to be a source of coarse-grained detritus for the Pahau depocentres.

8.2. Comparing igneous clasts with potential sources

The fact that the plutonic clasts are now found in conglomerates means that source regions must be

deeply eroded, i.e., that only the deeper levels of source igneous complexes, if they can be found, are now preserved in provenance areas. For example, all present outcrops of plutonic rocks within the MTZ expose equilibration depths of >5 km. However, Brown et al. (1998) demonstrated that granitoid clasts in Pleistocene–Holocene ignimbrites in the Taupo Volcanic Zone are geochemically and isotopically identical to penecontemporaneous rhyolite lavas and pyroclastic rocks erupted from the central Taupo Volcanic Zone. Their petrographic features are characteristic of mid- to high-level intrusions, with textures indicating hypersolvus and subsolvus crystallisation conditions. The Taupo Volcanic Zone clast REE patterns and Sr–Nd–Pb–O isotope ratios are comparable to published data from Taupo Volcanic Zone rhyolites. Brown et al. (1998) therefore proposed that the granitoid clasts represent crystallised portions of the magma chamber. By analogy, we consider it reasonable to compare volcanic and hypersolvus igneous clasts in Pahau conglomerates with deeper level exposures of penecontemporaneous igneous complexes in potential source regions.

8.3. Late Jurassic/Early Cretaceous clasts

The prevalence of volcanic and hypersolvus clasts in all conglomerates suggests active volcanism in the source area at the time of the Pahau sedimentation. However, with a few exceptions (Whitsunday Volcanics, Largs Ignimbrite), plutonic rocks dominate the SW Pacific igneous provinces described above.

8.3.1. Geochronology

The majority of U–Pb zircon ages for Pahau igneous clasts ($n = 11$, 147–134 Ma) match the ages of the Darran Suite and the Electric Granite of the MTZ, the Crow Granite of the Western Province and with igneous rocks on Thurston Island (Fig. 13). The 140 ± 2-Ma age of the Largs Ignimbrite is indistinguishable from dated rhyolitic Pahau clasts, e.g., those from Mount Saul. The three slightly younger clasts (128–123 Ma) show a strong overlap in age with the oldest dated Whitsunday Volcanics, with the Separation Point Suite of the MTZ, the Western Fiordland Orthogneiss, and the granitoids exposed on the Ruppert-Hobbs Coast, Pine Island Bay and Thurston Island.

8.3.2. Chemistry

For simplicity, the igneous clasts will now be subdivided into 'calc-alkaline clasts' and 'peralkaline clasts'. Potential clast sources with suitable bulk compositions (SiO_2>65%) have been combined into a 'felsic source' to simplify chemical comparison. The felsic source includes members of the Darran Suite, Separation Point Suite, Thurston Island, Marie Byrd Land, Te Kinga Suite and Whitsunday Volcanics. The felsic source is dominated by weakly peraluminous and metaluminous plutons; a few peraluminous plutons occur in the Te Kinga and Separation Point Suites (Fig. 4). Like the clasts, the 'felsic source' plots within the high-K calc-alkaline series.

All source suites show trends of decreasing Al_2O_3, Fe_2O_3, MgO, CaO with increasing SiO_2 and their felsic members (including the Largs Ignimbrite) show considerable overlap with the calc-alkaline clasts (Fig. 4). The peralkaline clasts have lower Al_2O_3 and higher TiO_2 and Fe_2O_3 than the felsic source and thus require a different provenance. The peralkaline Electric Granite (see above) appears to be an excellent match for these clasts. In addition to matching major element compositions, key trace elements (e.g., low Sr, high Zr–Nb, Fig. 5) are also similar.

Multi-element patterns for all clasts are enriched in incompatible large ion lithophile (LIL) elements and show pronounced Nb depletions; relative Sr abundances vary (Fig. 6A). LIL enrichment over LREE and Nb–Ti depletion is characteristic of arc magmatism, suggesting that the source for all igneous clasts is related to subduction. Average multi-element patterns of calc-alkaline igneous clasts correlate well with average trends for selected units of the felsic source (Fig. 8A). In Fig. 8B, comparison is made between rhyolitic clasts from Mount Saul and the calc-alkaline Largs Ignimbrite; this was prompted by the indistinguishable zircon ages of these felsic volcanics. The patterns match reasonably well. On the other hand, Largs Ignimbrite clearly cannot be a source for the peralkaline clasts with their pronounced depletions at Ba, Sr and Ti. Some Sr-enriched, HFSE-depleted Kekerengu clasts show patterns that are strikingly similar to those for averaged Separation Point Suite (Fig. 8C); the latter has adakitic affinities (Muir et al., 1995). Patterns for clasts classified as A-type from Mount Saul and Kekerengu are closely matched by the pattern for the Electric Granite, with marked negative

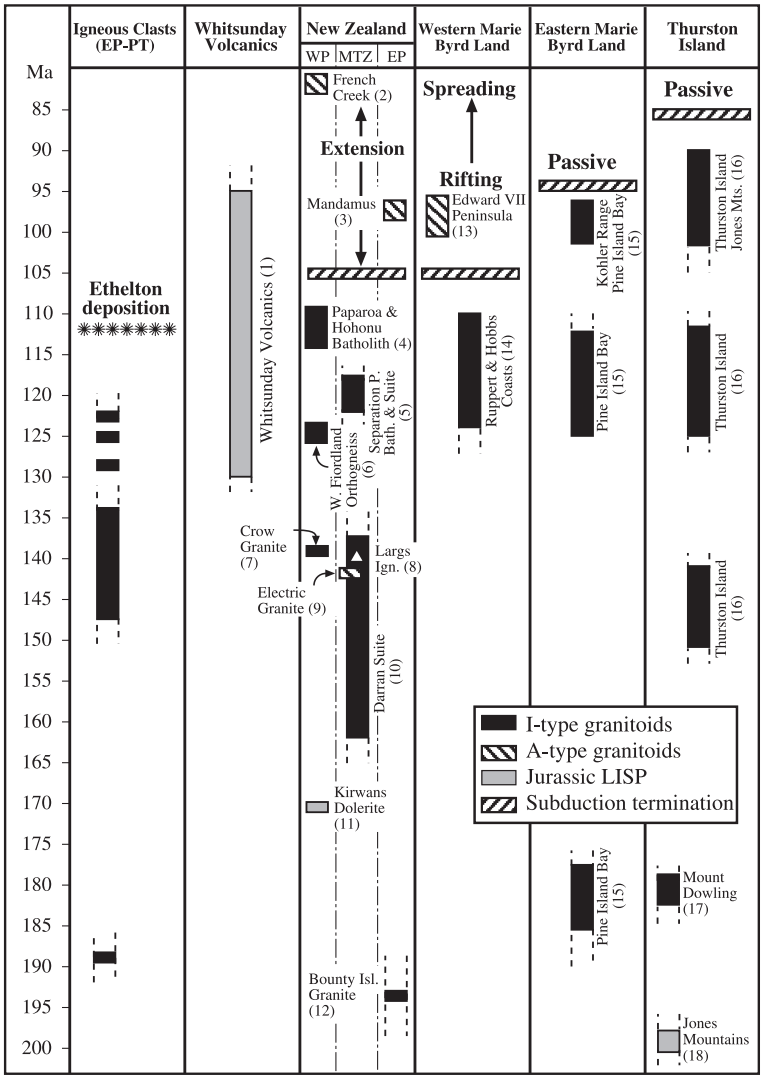

Fig. 13. Diagram showing west to east younging of the cessation of subduction-related magmatism (black), timing of rift magmatism (hatched) and large igneous silicic province related magmatism (medium grey) in Australia, New Zealand, Marie Byrd Land, and Thurston Island, compared with igneous clasts from the Eastern Province Pahau terrane = EP-PT. Localities or units are: WP = Western Province, MTZ = Median Tectonic Zone, EP = Eastern Province. Literature citations are: (1) Ewart et al. (1992), (2) Waight et al. (1998a), (3) Weaver and Pankhurst (1991), (4) Waight et al. (1998b), (5) Muir et al. (1998, 1995), (6) Muir et al. (1998), (7) Muir et al. (1997), (8) Mortimer (personal communication), (9) Muir et al. (1998), (10) Muir et al. (1998), (11) Mortimer et al. (1995), (12) Ireland (personal communication), (13) Weaver et al. (1994), (14) Pankhurst et al. (1993, 1998), Mukasa and Dalziel (2000), (15) Pankhurst et al. (1993, 1998), Pankhurst (personal communication), Mukasa and Dalziel (2000), (16) Pankhurst et al. (1993; 1998), Pankhurst (personal communication), Mukasa and Dalziel (2000), (17) Pankhurst et al. (1993, 1998), Pankhurst (personal communication), Mukasa and Dalziel (2000), (18) Pankhurst et al. (1993, 1998), Pankhurst (personal communication), Mukasa and Dalziel (2000).

anomalies at Ba, Sr and Ti, minor negative anomalies at Nb, and enrichment in HFS elements (Fig. 8D). This similarity also extends to the REE patterns (Fig. 6B).

On a Nb–Y plot (Pearce et al., 1984), the calc-alkaline clasts and the felsic source show almost complete overlap, both plotting predominantly in the

volcanic-arc-granite (VAG) field (Fig. 7). By contrast, the peralkaline clasts from Mount Saul and the single peralkaline clast from Kekerengu plot within the within-plate granite (WPG) field; again, the match with the peralkaline Electric Granite is clear.

8.3.3. Sr–Nd isotopes

For comparison purposes, initial Sr–Nd isotope ratios for the Late Jurassic–Early Cretaceous igneous clasts and for SW Pacific igneous provinces were calculated at 137 Ma (Fig. 14A and B). Sr and Nd isotope values for the Late Jurassic to Early Cretaceous source rocks from the Whitsunday Volcanics (Ewart et al., 1992), Median Tectonic Zone and Western Fiordland Orthogneiss (Muir et al., 1998), Separation Point Batholith (Muir et al., 1995), Hohonu Batholith (Waight et al., 1998b), Ruppert-Hobbs Coast and Pine Island (Pankhurst, personal

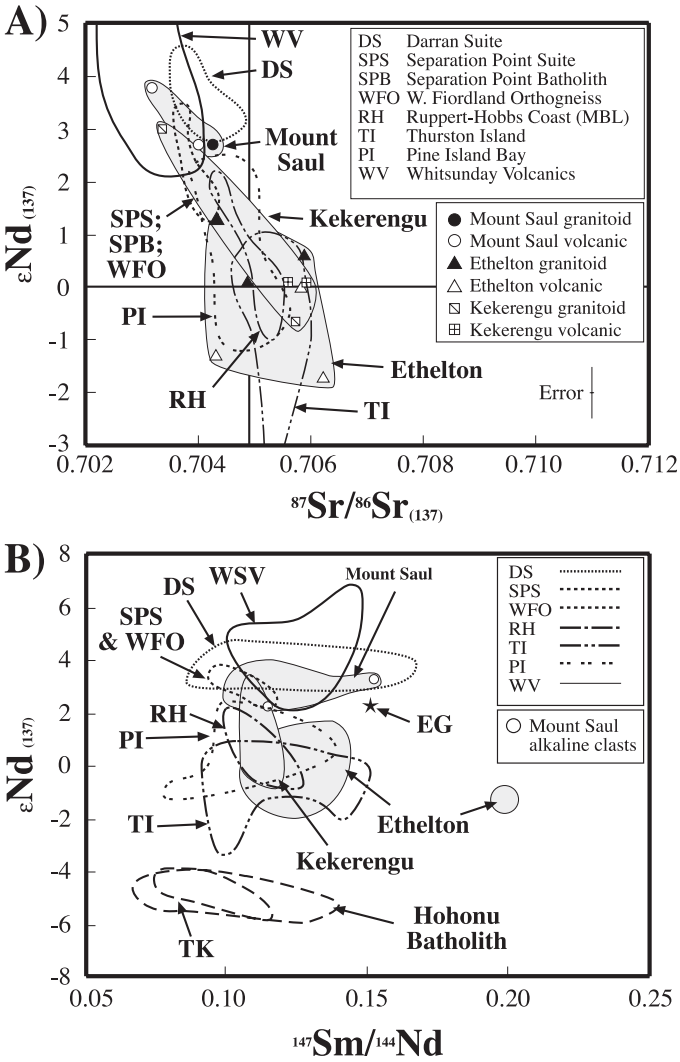

Fig. 14. $\varepsilon Nd_{(137)}$ versus $^{87}Sr/^{86}Sr_{(137)}$ and $\varepsilon Nd_{(137)}$ versus $^{147}Sm/^{144}Nd$ for igneous clasts compared with source rocks from the SW Pacific. Data for Whitsunday Volcanics (Ewart et al., 1992), the Separation Point Batholith, Separation Point Suite, Darran Suite and Western Fiordland Orthogneiss, Electric Granite (Muir et al., 1998, 1997, 1995), Hohonu Batholith (Waight et al., 1998b), Ruppert-Hobbs Coast and Pine Island (Pankhurst, personal communication) and Thurston Island (Pankhurst et al., 1993) all recalculated to 137 Ma, the mean age of all Pahau igneous clasts.

communication), and Thurston Island (Pankhurst et al., 1993) have been added in Fig. 14A and B for comparison.

The two youngest clasts with their high Rb/Sr and low Sr contents (Table 3) give unrealistically low $^{87}Sr/^{86}Sr_{(137)i}$ for these samples, therefore original $^{87}Sr/^{86}Sr_i$ values are plotted. Isotopic data for the felsic source form an extensive array over ≈ 10 εNd units: Whitsunday Volcanics, the Darran and Separation Point suites and the Western Fiordland Orthogneiss of Fiordland, and the Separation Point Batholith of NW Nelson have positive εNd whereas granitoids from the Antarctic sector (Ruppert-Hobbs Coast, Pine Island Bay, Thurston Island) extend to negative εNd. Pahau igneous clasts show extensive overlap with this isotopic array. In detail, clasts from Mount Saul are similar to the high-εNd source rocks whereas clasts from Ethelton and Kekerengu show wider ranges and overlap extensively with several members of the felsic source (Fig. 14A).

A similar pattern is observed on the $Nd_{(137)}$ vs. $^{147}Sm/^{144}Nd$ plot (Fig. 14B). The Sm/Nd ratio is here used as an additional provenance tracer (Fletcher et al., 1992; McLennan et al., 1990). The peralkaline Electric Granite, previously shown to closely match peralkaline clast compositions, also provides a close match isotopically; the Electric Granite (star) plots close to an peralkaline clast from Mount Saul. Granitoids from the ≈ 110 Ma Hohonu Batholith in the Western Province are too young and have an unsuitable εNd to be a source for the analysed clasts.

8.4. Early Jurassic clast

One of the Kekerengu igneous clasts, porphyritic granite UC30732, has an Early Jurassic U–Pb zircon age of 188 ± 3 Ma, some 40–50 Ma older than the other, compositionally similar clasts from this conglomerate. Potential sources for felsic igneous rocks of this age may be located on Bounty Island and in Antarctica (volcanics at Mount Dowling and V1 volcanics in Palmerland) or, as proposed by Pickard et al. (2000), in the region of the northern Lord Howe Rise or West Norfolk Ridge.

Available chemical data for potential Early Jurassic source rocks indicate that all these rocks plot in the high-K calc-alkaline field and are slightly peraluminous, with some of the high-Ti Palmerland volcanics and one of the low-Ti Palmerland volcanics being strongly peraluminous (Fig. 9A). As usual, TiO_2, Al_2O_3, Fe_2O_3, MgO, CaO and P_2O_5 abundances decrease with increasing SiO_2 (Fig. 9B), while Na_2O is scattered. Granites from the Bounty Island and Jones Mountains are indistinguishable from Kekerengu UC30732, and the low-Ti volcanics also show some similarities. The strongly differentiated composition of the clast (>77% SiO_2) means that its multi-element plot shows particularly strong depletions for some elements (e.g., Th, Sr, Ti) relative to potential sources (Fig. 9D) but the combination of low Sr and very high SiO_2 can still be found in some sources (e.g., Bounty Island, Fig. 9C). On the other hand, low-Sr granites such as those from the Jones Mountains have higher Rb and Nb, and lower Zr (Leat et al., 1993). All rocks from Palmerland have higher Zr-Nb concentrations relative to Kekerengu UC30732 (Riley et al., 2001). The good match with Bounty Island is confirmed by the Nb–Y plot (Fig. 9E) where both the clast and Bounty Island granites plot together in the field for volcanic arc granites.

Sr–Nd isotope ratios (all calculated at 188 Ma) show that some potential sources (e.g., Palmerland, Jones Mountains) are too high in $^{87}Sr/^{86}Sr$ compared with Kekerengu UC30732 (and all other clasts for that matter, Fig. 14) to be viable provenance candidates (Fig. 9F). The Mount Dowling volcanics do have broadly similar $^{87}Sr/^{86}Sr$ but εNd is too low. Some Early Jurassic granites from Pine Island Bay have broadly appropriate isotopic signatures but unfortunately no major and trace element data were available to test the compositional match. No isotopic data are available for Bounty Island.

8.5. Provenance of igneous clasts

Geochronological, major and trace element, and Sr–Nd isotope data define the subduction-related Median Tectonic Zone and Amundsen Province as the major Late Jurassic to Early Cretaceous source of the Pahau terrane igneous clasts.

Clasts from all three conglomerates are dominated by silicic and highly fractionated volcanic and granophyric, hypersolvus clasts. The paucity of volcanic rocks exposed in potential source areas today and the

ubiquitous presence of predominantly rhyolitic volcanic and hypersolvus granitoid clasts in the conglomerates is distinctive. This points strongly to the stripping and erosion of the upper levels of the Median Tectonic Zone and the Amundsen Province and the subsequent transportation to the place of final deposition.

Calc-alkaline clasts are geochemically indistinguishable from the Whitsunday Volcanics and the Mount Saul and Kekerengu clasts for which we have Sr–Nd isotope data show petrogenetic similarities with this volcanic province. The main period of volcanic activity occurred between ca. 120 and 95 Ma, coinciding with the youngest detrital zircon from the Ethelton matrix (111.7 ± 1.4 Ma) and approximately with the youngest dated igneous clasts and A-type magmatism along the Marie Byrd Land margin. The low relief, caldera-dominated Whitsunday Volcanic Province is generally too young in age to be a major clast source, although older equivalents might occur on the submerged Lord Howe Rise.

Many of the A-type clasts from Mount Saul and Kekerengu are indistinguishable in age, geochemistry and petrogenesis from the Electric Granite of the MTZ. The Electric Granite is therefore proposed as the clast source.

The majority of the calc-alkaline clasts from all three conglomerates are indistinguishable in age, chemical composition and petrogenesis from the calc-alkaline I-type granitoids of the Darran Suite and the Thurston Island granitoids from Marie Byrd Land. Calc-alkaline clasts with adakitic affinities from Kekerengu can geochemically best be correlated with the Separation Point Suite, and these rocks are deemed to be the adakitic source. The Hohonu Batholith is generally too young in age and isotopically too radiogenic relative to the clasts.

The inferred presence of both Darran Suite and Separation Point-type derived clasts at Kekerengu and of the Electric Granite derived clasts at Mount Saul is distinctive. Furthermore, the similar petrogenesis of A-type clasts from Kekerengu and Mount Saul and of I-type clasts from all three conglomerate locations is noteworthy. If the close proximity (present geography) of the three conglomerate locations is considered, then this might suggest that all three conglomerate locations were derived from a relatively narrow sector of the Median Tectonic Zone where the Darran Suite, the Separation Point-type rocks and the Electric Granite were in close proximity. The granitoids of the Darran Suite are proposed as the main source of calc-alkaline clasts. The geographic separation between the Thurston Island crustal block and the New Zealand sector of an Early Cretaceous (Aptian) Panthalassan margin configuration (see below and Fig. 16) indicates that the granitoids of Thurston Island might be too distal (with respect to the Pahau depositional basins) in order to supply pebble to boulder-sized clasts.

Based on the available geochronological and geochemical data presented above the Early Jurassic calc-alkaline I-type clast from Kekerengu is best correlated with granitoids exposed on the Bounty Island and in Pine Island Bay. Although the geochemical data record of the Bounty Island and Pine Island Bay granitoids is incomplete, the available data show that the age and petrogenesis of the Pine Island Bay granites and the age and geochemistry of the Bounty Island granites are indistinguishable from that of this single clast.

The calc-alkaline Mount Dowling andesites are geochemically too mafic and isotopically too radiogenic to be a viable source for the clast. The pene-contemporaneous Jones Mountains calc-alkaline S-type granitoids and the volcanics from Palmerland are isotopically too radiogenic relative to the clast and display mixed geochemical signatures consistent with emplacement into an intra-plate environment.

8.6. Pahau sandstone clasts-recycled Rakaia terrane

Several lines of evidence presented here and suggested by others (e.g., MacKinnon, 1983; Roser and Korsch, 1999; Smale, 1997) strongly supports earlier claims that Pahau depocentres received detritus recycled from older Torlesse rocks in the inboard Rakaia terrane. The Otago Schist is the first regional metamorphic event recognised in the Rakaia terrane and is attributed to the Caples-Torlesse terrane collision (e.g., Mortimer, 1993, and references therein). Rapid cooling of the Otago Schist between 140 and 130 Ma has been interpreted by Little et al. (1999) as a signal of uplift, thereby making Rakaia terrane material available for erosion. Sandstone clasts collected at Ethelton and Mount Saul show strong petrographic similarities to Rakaia sandstones (Fig. 10) and no similarities with sandstones from other terranes (e.g., Caples, Maitai, Murihiku or Brook Street). This similarity with Rakaia

sandstones is confirmed by the geochemistry of most clasts (Fig. 11A and B). In detail, some of the Ethelton sandstone clasts plot in the volcanic terrane (VT field) which indicates the availability of mafic volcanic material in the original provenance of the recycled sandstones clasts. The clasts in the VT field have some of the highest mafic mineral contents of all sandstone clasts and this is reflected in high Sc and low Th concentrations. This suggests that sandstones of a more primitive nature were accessible for erosion. In the SiO_2/Al_2O_3–Th/Sc plot used to define the fields originally these clasts from Ethelton plot in the same area as some of the Caples sandstones (Roser and Korsch, 1999, their Fig. 8A).

Zircon U–Pb age patterns lend further support to the importance of recycled Rakaia materials. Most importantly, the major detrital zircon age peak (250–200 Ma) present in Triassic Rakaia and Waipapa/Caples sandstones is also found in the Aptian Ethelton sandstone matrix (Fig. 12). Two minor age groups (300–280 Ma; 340–320 Ma) at Ethelton also coincide with peaks in Permian and Carboniferous Rakaia sandstones. Finally, minor Ordovician and Precambrian age components in the Ethelton sample are also found in both Rakaia and Waipapa/Caples terrane rocks, whereas the minor Devonian peak in the Ethelton sandstone is absent in the older terranes. Clearly, material with a major Triassic and various minor Paleozoic detrital zircon components was recycled from the older inboard Rakaia and Waipapa/Caples terranes into Early Cretaceous Pahau depocentres.

Other zircon evidence is equally important: Early Jurassic age peaks in the Waipapa/Caples terrane are also recognised in the Ethelton matrix (and other Pahau sandstones). Furthermore, one of the Kekerengu igneous clasts has an Early Jurassic zircon age. The latter could originate from granites on Bounty Island and Pine Island Bay. The Early Jurassic zircon age peak also broadly coincides with the Jurassic age proposed for docking of the Caples and Rakaia terranes.

8.7. Pahau sandstone provenance

Biostratigraphic age constraints for the Pahau terrane conglomerates agree broadly with U–Pb zircon ages from igneous clasts and detrital zircons from our study. Biostratigraphy indicates an Albian sedimentation age for the Kekerengu and an Aptian age for the Mount Soul conglomerates. Continuation into the Aptian is also indicated for Ethelton based on its youngest detrital zircon (111.7 ± 1.4 Ma). The pronounced Early Cretaceous zircon age peak in the Ethelton matrix (140–120 Ma) broadly coincides with the narrow age range for the igneous clasts (Fig. 12), suggesting that igneous activity in the source of both the detrital zircons (in sandstones) and the igneous clasts was essentially contemporaneous with sediment deposition. However, the main element chemistry of igneous clasts in the conglomerates differs from that of Pahau terrane sandstones, implying that the igneous clast source cannot be the sole source of the Pahau sandstones. On a comparative plot (Fig. 11A), most clasts are distinctly different in composition from the sandstones, with the majority of the clasts being of evolved rhyolitic and dacitic composition.

Sr–Nd isotope ratios (at 137 Ma) for all but one Pahau sandstone lie between the fields defined by the igneous clasts and the Rakaia sandstones (Fig. 11C). This indicates that neither the igneous clast source nor the Rakaia sandstones, by themselves, would be suitable sources for many Pahau sandstones. On the other hand, Pahau sandstones could represent mixtures of recycled older Rakaia and Caples terrane sandstones with igneous clast-type material derived from an active arc also suggested by Roser and Korsch (1999).

The feasibility of such a mixed origin can be tested by combining isotopic and trace element constraints. Here we employ Th–Sc elemental and Nd isotopic systematics (McLennan and Hemming, 1992; McLennan et al., 1990; Roser and Korsch, 1999; Wombacher and Münker, 2000). Available Nd isotope and Th/Sc compositions for the SW Pacific igneous provinces are plotted in Fig. 15 and are compared with compositions of Pahau and Rakaia terrane sandstones and other Eastern Province terranes of New Zealand. Based on biostratigraphic age constraints and the youngest detrital zircons from the Ethelton matrix, the notional depositional age for the Pahau terrane sandstones is taken as 115 Ma and all ε_{Nd} values are calculated at this age.

The recycling of Caples and Rakaia sandstone with a possible minor contribution from the Median Tec-

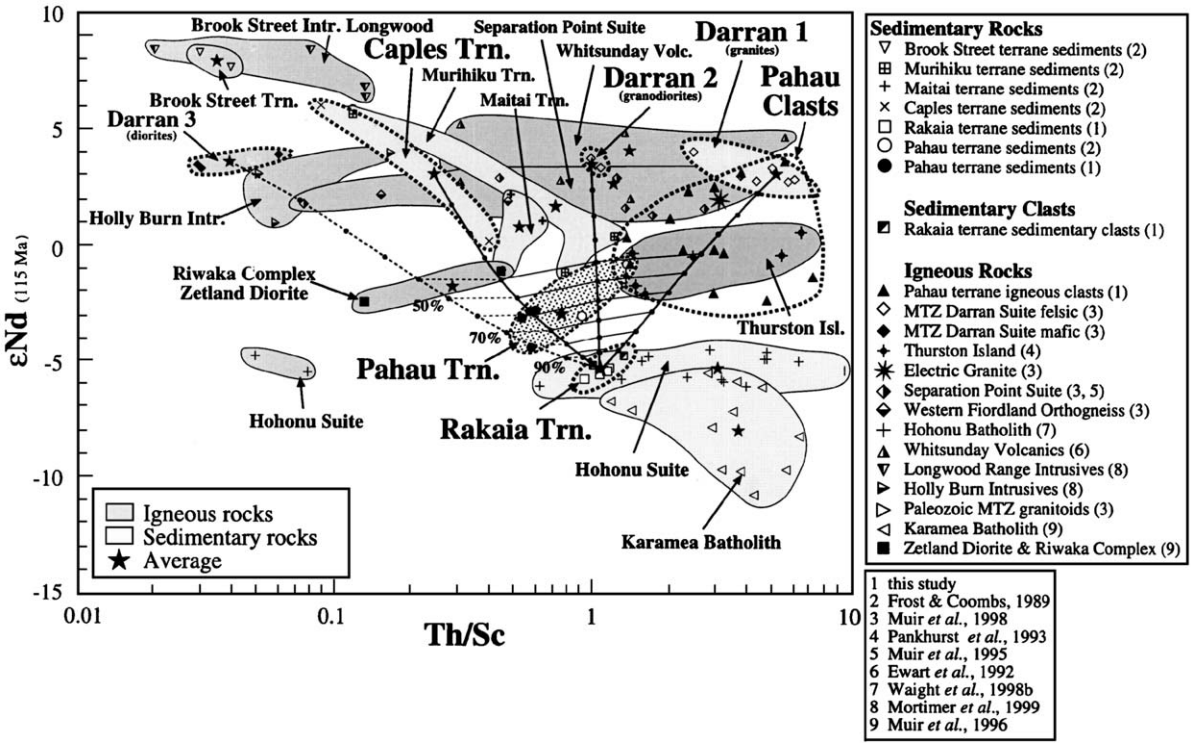

Fig. 15. $\varepsilon Nd_{(115)}$ versus Th/Sc for igneous clasts compared with Eastern Province terrane sediments and igneous rocks from the Panthalassan margin provinces. Th and Sc trace element data for the Torlesse terranes are from this study, those for the Murihiku terrane are from Roser et al. (2000) and those for the Brook Street, Maitai and Caples terranes from Roser (personal communication). Dots on mixing line indicate 10% mixing steps. Average composition (star) used: Rakaia (Th = 11 ppm, Sc = 10 ppm, Th/Sc = 1.1, Nd = 27 ppm, εNd = − 5.3), Darran 1 (Th = 21 ppm, Sc = 4 ppm, Th/Sc = 5.25, Nd = 25 ppm, εNd = 3.2), Darran 2 (Th = 8 ppm, Sc = 8 ppm, Th/Sc = 1.0, Nd = 19 ppm, εNd = 3.6), Darran 3 (Th = 1 ppm, Sc = 33 ppm, Th/Sc = 0.03, Nd = 13 ppm, εNd = 3.6), Caples (Th = 5 ppm, Sc = 20 ppm, Th/Sc = 0.25, Nd = 15 ppm, εNd = 3.1).

tonic Zone was proposed by Roser and Korsch (1999) to explain the Pahau sandstone composition. Results from our work show that an active volcanic arc contributed detritus to the Pahau basin and that at least three or more sources are required to produce the Pahau sandstones. Assuming simple bulk mixing between Rakaia detritus and detritus derived from the igneous sources and other Eastern Province terranes, and that no significant trace element fractionation took place, crude and tentative estimates of detritus contributions of the various end-members can be obtained.

The Pahau sandstones display a wide range of compositions ranging from intermediate to felsic. Although part of the intermediate Pahau composition can be explained by a simple Rakaia–Caples mixing, there is a spread of the Pahau range toward the igneous clast source with a minor overlap between the Pahau sandstone and the igneous clast fields. This indicates that a silicic igneous contribution is more significant in some Pahau sandstones. These more felsic compositions could best be explained by mixing 40–60% Rakaia material and 60–40% Caples–Darran 2 detritus (Jackson Peak and Mount Luxmore granodiorites). The source for the more mafic Pahau detritus is more ambiguous and cannot be explained by the mixing of Rakaia–Caples detritus. Although no mafic igneous clasts were found in this work such clasts have been found in other locations from the Pahau terrane (e.g., Clarence River, Mazengarb, personal communication). In addition, plagioclase of andesine composition has been reported from Pahau sandstones (MacKinnon, 1980). This may indicate that clasts of mafic and intermediate composition have

disintegrated and are now part of the Pahau sandstone. Conversely, andesine has also been reported by Grapes et al. (2001) from the Rakaia and Caples sandstones. The andesine could have been derived from the disintegration of these rocks. If the felsic Darran members contributed detritus to the Pahau basin, then it is reasonable to assume that the contemporaneous mafic Darran member also contributed detritus. The most mafic Pahau sandstones could best be explained by a mixture of 70–80% Rakaia detritus and 30–20% Caples–Darran 3 material. The contrast between individual potential source provinces indicates that the volumetric contribution of the igneous clast source was relatively minor, and that most of the detritus in the Pahau turbidites were derived from the Caples Rakaia terrane as suggested by Roser and Korsch (1999).

There are various other mafic source rocks that could have contributed detritus by erosion to the Pahau basin, including the Brook Street terrane, and the Longwood and Holly Burn Intrusives. Detritus contribution by the Maitai and Murihiku terranes is a possibility. That the Murihiku basin received detritus not only from the Maitai/Caples terranes, but also from the Median Tectonic Zone to the west is indicated by the presence of MTZ-like igneous clasts in the Murihiku terrane (Graham and Korsch, 1990). Furthermore, the detritus shed from the MTZ and the Maitai/Caples terranes is broadly similar in composition (εNd) to that of the Murihiku terrane, as shown in Fig. 15.

However, if offshore borehole (Waimamaku-2) interpretations by Isaac et al. (1994) are correct (bottom of core interpreted as Murihiku), then the Murihiku terrane is still a depositional basin (sediment trap) at the time of the Pahau sandstone deposition and cannot be a major contributor of detritus. Initial sediment supply from the MTZ to the Pahau basin was accompanied by the uplift of the combined Rakaia/Caples/Maitai terranes (Little et al., 1999), giving rivers the opportunity to continuously incise and transect the emerging mountain range. While small rivers contributed detritus from the MTZ and Rakaia/Caples/Maitai to the Murihiku basin large rivers in the South Island region transported MTZ-derived detritus across the slowly uplifting Murihiku basin, while the North Island sector was still a depositional basin.

8.8. Regional tectonic implications

The tectonic regime in the South Island New Zealand region changed from subduction-related processes to extension at ca. 105 Ma (Bradshaw, 1989; Luyendyk, 1995; Spell et al., 2000). The youngest U–Pb dated igneous clast from the Pahau terrane is a subsolvus/hypersolvus monzogranite (UC30743; containing minor granophyric intergrowth) that gave an age of 123.1 ± 2.5 Ma. The youngest detrital zircon dated from the Ethelton matrix gave an age of 111.7 ± 1.4 Ma. This age constrains the minimum age of magmatism in the source region of the Pahau terrane.

The Aptian reconstruction of the New Zealand sector of the Panthalassan Gondwana margin (Fig. 16) is adapted from that proposed by Mukasa and Dalziel (2000) but was modified by removing the dextral displacement proposed by DiVenere et al. (1995) between the eastern and western Marie Byrd Land crustal blocks (Ross and Amundsen Province of Pankhurst et al., 1998). This modification is based on the following observations:

(i) The LeMay Group of Alexander Island, Antarctic Peninsula, is a Mesozoic accretionary prism constructed during subduction of Pacific ocean floor and the Phoenix plate (Doubleday et al., 1993; Holdsworth and Nell, 1992; McCarron and Larter, 1998; Tranter, 1992). Radiolaria biostratigraphy constrains its depositional age range from latest Jurassic to at least Albian (Holdsworth and Nell, 1992). If sedimentation of the LeMay Group continued at least into the Albian, then the positioning of the Thurston Island block in front of Alexander Island in the Barremian reconstruction of Mukasa and Dalziel (2000, their Fig. 9A) is questionable. In our reconstruction, the Thurston Island, eastern Marie Byrd Land and eastern Campbell Plateau blocks (Mukasa and Dalziel terms) have been moved sinistrally, thereby removing the strike slip separation between the Marie Byrd Lanap' between the Campbell and Challenger plateaux.

(ii) The strike-slip separation proposed by DiVenere et al. (1995) is based on paleomagnetic data from granitoids and volcanics along the Ruppert

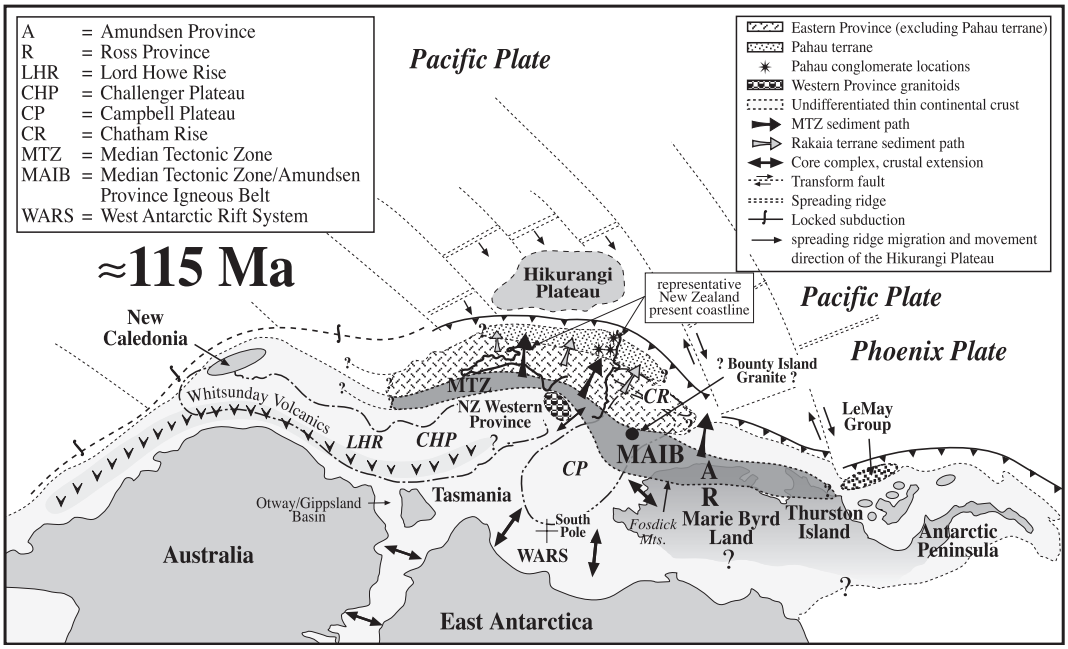

Fig. 16. Early Cretaceous reconstruction of Gondwana indicating the main features discussed in the text. Amundsen Province (AP) and Ross Province (RP) of Pankhurst et al. (1998) are juxtaposed next to each other. South Pole and crustal block configuration adapted from Mukasa and Dalziel (2000), but the displacement between the Amundsen and Ross Provinces, proposed by DiVenere et al. (1995), has been removed.

Coast, including areas adjacent to the core complex structure in the Fosdick Mountains of the Ford Ranges (Luyendyk et al., 1996). Movement associated with the core complex and a zone of continental separation may have caused postmagnetisation rotation of the measured poles. This may account for paleopoles that require strike-slip displacement and the placement of the Thurston Island crustal block in front of the accretionary complex while accretion was still taking place.

(iii) One of the most striking features on the present-day Campbell Plateau is a northeast tending zone of high amplitude positive magnetic anomalies, termed the Campbell Magnetic Anomaly System (Davey and Christoffel, 1978). The gravity and the magnetic anomalies indicate a major geological feature underlying the area, but its possible correlation with known tectonic zones (Median Tectonic Zone, Amundsen Province) is uncertain (Sutherland, 1999). If Bounty Island is part of the MTZ (Cook et al., 1999), then the Campbell Magnetic Anomaly System may represent MTZ (and Western Province?) correlatives intruded into the Campbell Plateau. Bradshaw et al. (1997) proposed similar paleo-relationships. Our reconstruction therefore shows MTZ extending across Campbell Plateau to join with Amundsen Province correlatives, forming what we term the Median Tectonic Zone/Amundsen Province igneous belt (MAIB).

(iv) The continuity of the Campbell Magnetic Anomaly System across the entire central Campbell Plateau removes the need for major strike-slip displacement between the Eastern and Western Campbell plateaux as proposed by Mukasa and Dalziel (2000), and lends further support to the crustal block arrangement presented here.

(v) It has been suggested that the Torlesse terranes are ‘exotic’ (DiVenere et al., 1995; Pickard et al., 2000). In the Great South Basin (Fig. 1), non-marine graben-fill successions overlie basement rocks of the Eastern Province (Beggs, 1993). Pollen from a drill hole gives Cenoma-

nian ages (Raine et al., 1993). However, the seismic interpretation indicates that ca. 1000 m of older sediments lie between the drill hole and the basement and an Albian age is possible. Therefore, the terranes of the Eastern Province were in place at ca. 105 Ma. There is no control on the juxtaposition of the Pahau terrane to the inboard Eastern Province terranes. The Pahau terrane was cut by the within-plate Mandamus Suite by ac. 100 Ma (Weaver and Pankhurst, 1991), and related lamprophyric dikes cut the Esk Head Melange. Therefore, scope for an exotic Cretaceous segment of the Pahau, as proposed by DiVenere et al. (1995), is limited.

The reconstruction shown in Fig. 16 provides explanations for a number of geological observations. For example, the map suggests a close proximity of several Early Cretaceous conglomerate locations, including those studied here and those in the Early Albian Waihere Formation, which unconformably overlies the Rakaia terrane basement on the Chatham Islands (Mildenhall, 1977). Granitoid clasts from the Chatham Island conglomerates analysed by Dean (1993) show many similarities with their counterparts in the conglomerates studied here. In particular, some A-type granitoid clasts from the Chatham Island conglomerates strongly resemble the A-type volcanic clasts from Mount Saul and Kekerengu. Assuming therefore that these similar-aged conglomerates were once close together, their present separation may be related to attenuation and stretching of thick continental crust in response to extension (e.g., Mukasa and Dalziel, 2000; Sutherland, 1999), prior to the actual separation between New Zealand and West Antarctica.

Calc-alkaline clasts in our Pahau conglomerates are geochemically indistinguishable from the Whitsunday Volcanics (Ewart et al., 1992); this is confirmed by Sr–Nd isotope data for the clasts from Mount Saul and Kekerengu (Fig. 14). Although the rift-related Whitsunday Volcanic Province is considered to be too young for the igneous clasts the age of the volcanics (125–95 Ma, Bryan et al., 2000; Ewart et al., 1992) was penecontemporaneous with sedimentation in the Pahau basins and with extension-related magmatism recorded in Marie Byrd Land (105–95 Ma , Storey et al., 1999). The presence of Whitsunday Volcanic Province-derived volcanoclastic sediments in the Otway/Gippsland Basin (Bryan et al., 1997) strongly indicates that the Whitsunday Volcanic Province extended into what is now the Lord Howe Rise. The possible extension of the Whitsunday Volcanic Province into the New Zealand region (Challenger Plateau) is shown in Fig. 16.

9. Conclusions

A detailed sampling program of igneous clasts from three Pahau terrane conglomerates and tectonostratigraphic constraints have helped to broadly characterise the igneous protosources of the Pahau terrane.

Geochronological, major and trace element, and Sr–Nd isotope data from the Pahau terrane igneous clasts indicate that subduction-related magmas were intruded into an active continental margin. All the clasts display a general concordance that suggests a similar petrogenesis and derivation from a single suite, except for the peralkaline clasts from Mount Saul and Kekerengu. The Late Jurassic to Early Cretaceous calc-alkaline, metaluminous to weakly peraluminous clasts are indistinguishable in age, chemical composition, and petrogenesis from the felsic members of the calc-alkaline I-type granitoids of the Darran Suite, whereas the peralkaline rhyolitic clasts from Mount Saul and Kekerengu correlate best with the Electric Granite. The Darran Suite and the Electric Granite are part of the Median Tectonic Zone, and the subduction-related MTZ/Amundsen Province igneous belt is therefore proposed as the source for Pahau terrane igneous clasts.

The clast populations from all three Pahau conglomerates are dominated by silicic and highly fractionated volcanic and granophyric, hypersolvus clasts. The presence of these lithotypes is attributed to the stripping and erosion of the upper levels of the MAIB and the subsequent transportation to the place of final deposition.

Most of the igneous clast ages from Ethelton and Kekerengu overlap with the Early Cretaceous detrital zircon age group of the Ethelton conglomerate sandstone matrix, indicating that sedimentation and source magmatism were penecontemporaneous. The youngest detrital zircon dated from the matrix gives an age

of 111.7 ± 1.4 Ma that constrains the minimum age of magmatism in the source region of the Pahau terrane and the age of sedimentation.

The Early Jurassic clast from Kekerengu correlates with the calc-alkaline, weakly peraluminous Bounty Island Granite, which shares a similar petrogenetic history with the contemporaneous Pine Island granitoids, suggesting that the Campbell Plateau was in close proximity to Thurston Island/Marie Byrd Land in the Early to Middle Jurassic.

Acknowledgements

The authors like to thank Doug Coombs for providing rock samples, Barry Roser for unpublished sandstone data and Bob Pankhurst for unpublished isotope data. This paper represents part of a PhD thesis by the principal author funded by a scholarship at the University of Canterbury. The costs of field and laboratory work were partially funded by the Mason Trust and a University of Canterbury research grant.

References

Adams, C.J., Graham, I.J., 1996. Metamorphic and tectonic geochronology of the Torlesse terrane, Wellington, New Zealand. New Zealand Journal of Geology and Geophysics 39 (2), 157–180.

Adams, C.J., Kelley, S., 1998. Provenance of Permian–Triassic and Ordovician metagraywacke terranes in New Zealand: evidence from Ar-40/Ar-39 dating of detrital micas. Geological Society of America Bulletin 110 (4), 422–432.

Allen, C.M., Williams, I.S., Stephens, C.J., Fielding, C.R., 1998. Granite genesis and basin formation in an extensional setting: the magmatic history of the northernmost New England Orogen. Australian Journal of Earth Sciences 45 (6), 875–888.

Andrews, P.B., Speden, I.G., Bradshaw, J.D., 1976. Lithological and paleontological content of the Carboniferous–Jurassic Canterbury Suite, South Island, New Zealand. New Zealand Journal of Geology and Geophysics 19 (6), 791–819.

Barnes, P.M., 1990. Provenance of Cretaceous accretionary wedge sediments: the Mangapokia Formation, Wairarapa, New Zealand. New Zealand Journal of Geology and Geophysics 33 (1), 125–135.

Bassett, K.N., 2000. Isotopic provenance analysis and terrane tectonics: a warning about sediment transport distances. In: Skilbeck, C., Hubble, T.C. (Eds.), Understanding Planet Earth: Searching for a Sustainable Future. Abstracts of the 15th Australian Geological Convention. University of Technology, Sydney, NSW, Australia, p. 24.

Beggs, J.M., 1993. Depositional and tectonic history of the Great South Basin. In: Ballance, P.F. (Ed.), South Pacific Sedimentary Basins. Sedimentary Basins of the World, vol. 2. Elsevier, Amsterdam, pp. 365–373.

Bishop, D.G., Bradshaw, J.D., Landis, C.A., 1983. Provisional terrane map of South Island, New Zealand. In: Howell, G., Jones, D., Cox, A., Nur, A. (Eds.), Proceedings of the Circum-Pacific Terrane Conference. Stanford University Publications. Geological Sciences. Stanford University, School of Earth Sciences, Stanford, CA, USA, pp. 24–31.

Bradshaw, J.D., 1973. Allochthonous Mesozoic fossil localities in melange in the Torlesse Group of North Canterbury. Journal of the Royal Society of New Zealand 3 (2), 161–167.

Bradshaw, J.D., 1989. Cretaceous geotectonic pattern in the New Zealand Region. Tectonics 8, 803–820.

Bradshaw, J.D., Adams, C.J., Andrews, P.B., 1981. Carboniferous to Cretaceous on the Pacific margin of Gondwana; the Rangitata phase of New Zealand. In: Cresswell, M., Vella, P. (Eds.), Gondwana Five; Selected Papers and Abstracts of Papers Presented at the Fifth International Gondwana Symposium. A.A. Balkema, Rotterdam, Wellington, New Zealand, pp. 217–221.

Bradshaw, J.D., Weaver, S.D., Pankhurst, R.J., Storey, B.C., Muir, R.J., 1997. New Zealand superterranes recognized in Marie Byrd Land and Thurston Island. Terra Antarctica 3, 429–436.

Brown, S.J.A., Burt, R.M., Cole, J.W., Krippner, S.J.P., Price, R.C., 1998. Plutonic lithics in ignimbrites of Taupo Volcanic Zone, New Zealand: sources and conditions of crystallisation. Chemical Geology. Isotope Geoscience Section 148, 21–41.

Bryan, S.E., et al., 1997. Early Cretaceous volcano-sedimentary successions along the Eastern Australian continental margin: implications for the break-up of Eastern Gondwana. Earth and Planetary Science Letters 153 (1–2), 85–102.

Bryan, S.E., Ewart, A., Stephens, C.J., Parianos, J., Downes, P.J., 2000. The Whitsunday volcanic province, central Queensland, Australia: lithological and stratigraphic investigations of a silicic-dominated large igneous province. Journal of Volcanology and Geothermal Research 99 (1–4), 55–78.

Campbell, J.D., Warren, G., 1965. Fossil localities of the Torlesse group in the South Island. Transactions of the Royal Society of New Zealand. Geology 3 (8), 99–137.

Cawood, P.A., Nemchin, A.A., Leverenz, A., Saeed, A., Ballance, P.F., 1999. U/Pb dating of detrital zircons: implications for the provenance record of Gondwana margin terranes. Geological Society of America Bulletin 111 (8), 1107–1119.

Coney, P.J., Edwards, A., Hine, R., Morrison, F., Windrim, D., 1990. The regional tectonics of the Tasman orogenic system, eastern Australia. Journal of Structural Geology 12, 519–543.

Cook, R.A., Sutherland, R., Zhu, H., 1999. Cretaceous–Cenozoic geology and petroleum systems of the Great South Basin, New Zealand. Institute of Geological and Nuclear Sciences Monograph, vol. 20. Institute of Geological and Nuclear Sciences, Lower Hutt, New Zealand. 188 pp.

Coombs, D.S., et al., 1976. The Dun Mountain Ophiolite Belt, New Zealand, its tectonic setting, constitution and origin, with special reference to the southern portion. American Journal of Sciences 276, 561–603.

Cooper, R.A., 1989. Early Paleozoic terranes of New Zealand. Journal of the Royal Society of New Zealand 19 (1), 73–112.

Davey, F.J., Christoffel, D.A., 1978. Magnetic anomalies across Campbell Plateau, New Zealand. Earth and Planetary Science Letters 41 (1), 14–20.

De Paolo, D.J., Wasserburg, G.J., 1976. Nd isotopic variations and petrogenetic models. Journal of Geophysical Research 3, 249–252.

Dean, A.A., 1993. Analysis and correlation of igneous clast geochemistry and petrography from four Mesozoic Conglomerates. Unpublished MSc Thesis, University of Canterbury, Christchurch, New Zealand, 263 pp.

DiVenere, V., Kent, D.V., Dalziel, I.W.D., 1995. Early Cretaceous paleomagnetic results from Marie Byrd Land, West Antarctica: implications for the Weddellia collage of crustal blocks. Journal of Geophysical Research B, Solid Earth and Planets 100 (5), 8133–8151.

Doubleday, P.A., MacDonald, D.I.M., Nell, P.A.R., 1993. Sedimentology and structure of the trench-slope to forarc basin transition in the Mesozoic Alexander Island, Antarctica. Geological Magazine 130, 737–754.

Eby, G.N., 1984. Monteregian Hills: 1. Petrography, major and trace element chemistry of the western intrusions: Mounts Royal, St. Bruno and Johnson. Journal of Petrology 25, 421–452.

Eby, G.N., 1990. The A-type granitoids: a review of their occurrence and chemical characteristics, and speculations on their petrogenesis. Lithos 26, 115–134.

Ewart, A., Schon, R.W., Chappell, B.W., 1992. The Cretaceous volcanic–plutonic province of the central Queensland (Australia) coast: a rift related ''calc-alkaline'' province. In: Brown, E., Chappell, B.W. (Ed.), The Second Hutton Symposium on the Origin of Granites and Related Rocks; Proceedings. Special Paper-Geological Society of America. Geological Society of America (GSA), Boulder, CO, USA, pp. 327–345.

Ferguson, R., Hoey, T., Wathen, S., Werritty, A., 1996. Field evidence for rapid downstream fining of river gravels through selective transport. Geology 24, 179–182.

Fletcher, I.R., Paul, D.K., Trendall, A.F., 1992. Sm–Nd and geochemical characteristics of metasedimentary rocks at Mt. Narryer, Western Australia. Australian Journal of Earth Sciences 39, 67–78.

Floettmann, T., Gibson, G.M., Kleinschmidt, G., 1993. Structural continuity of the Ross and Delamerian orogens of Antarctica and Australia along the margin of the paleo-Pacific. Geology 21 (4), 319–322.

Foster, D.A., Gray, D.R., 2000. Evolution and structure of the Lachlan fold belt (orogen) of eastern Australia. Annual Review Earth and Planetary Sciences 28, 47–80.

Frost, C.D., Coombs, D.S., 1989. Nd isotope character of New Zealand sediments: implications for terrane concepts and crustal evolution. American Journal of Science 289, 744–770 (June).

George, A.D., 1992. Deposition and deformation of an Early Cretaceous trench-slope basin deposit, Torlesse terrane, New Zealand. Geological Society of America Bulletin 104 (5), 570–580.

Gibson, G.M., Ireland, T.R., 1996. Extension of Delamerian (Ross) orogen into western New Zealand—evidence from zircon ages and implications for crustal growth along the Pacific margin of Gondwana. Geology 24 (12), 1087–1090.

Gibson, G.M., McDougall, I., Ireland, T.R., 1989. Age constraints on metamorphism and the development of a metamorphic core complex in Fiordland, southern New Zealand; reply. Geology 17 (4), 381–382.

Graham, I.J., Korsch, R.J., 1990. Age and provenance of granitoid clasts in Moeatoa Conglomerate, Kawhia Syncline, New Zealand. Journal of the Royal Society of New Zealand 20 (1), 25–39.

Grapes, R., Roser, B.P., Kashai, K., 2001. Composition of monocrystalline detrital and authigenic minerals, metamorphic grade, and provenance of Torlesse and Waipapa greywacke, Central North Island, New Zealand. International Geology Review 43, 139–175.

Holdsworth, B.K., Nell, P.A.R., 1992. Mesozoic radiolarian faunas from the Antarctic Peninsula: age, tectonic and paleo-oceanographic significance. Journal of the Geological Society, London 149 (Part 6), 1003–1020.

Howell, D.G., 1980. Mesozoic accretion of exotic terranes along the New Zealand segment of Gondwanaland. Geology 8 (10), 487–491.

Ireland, T.R., 1992. Crustal evolution of New Zealand: evidence from age distributions of detrital zircons in Western Province paragneisses and Torlesse greywacke. Geochimica et Cosmochimica Acta 56, 911–920.

Ireland, T.R., Floettmann, T., Fanning, C.M., Gibson, G.M., Preiss, W.V., 1998. Development of the early Paleozoic Pacific margin of Gondwana from detrital-zircon ages across the Delamerian Orogen. Geology 26 (3), 243–246.

Isaac, M.J., Herzer, R.H., Brook, F.J., Hayward, B.W., 1994. Cretaceous and Cenozoic sedimentary basins of Northland, New Zealand. Institute of Geological and Nuclear Sciences, Monograph, vol. 8. Institute of Geological and Nuclear Sciences, Lower Hutt, New Zealand. 204 pp.

Johnston, M.R., Raine, J.I., Watters, W.A., 1987. Drumduan Group of East Nelson, New Zealand; plant-bearing Jurassic arc rocks metamorphosed during terrane interaction. Journal of the Royal Society of New Zealand 17 (3), 275–301.

Jones, P.J., 1995. AGSO Phanerozoic Timescale: Wallchart and Explanatory Notes. Oxford Univ. Press, Melbourne, Australia, p. 32.

Kimbrough, D.L., et al., 1994. Uranium–lead zircon ages from the Median Tectonic Zone, South Island, New Zealand. New Zealand Journal of Geology and Geophysics 37 (4), 393–419.

Kodama, Y., 1994. Downstream changes in the lithology and grain size of fluvial gravels, the Watarase River, Japan: evidence of the role of abrasion in downstream fining. Journal of Sedimentary Research A64, 68–75.

Korsch, R.J., Wellman, H.W., 1988. The geological evolution of New Zealand and the New Zealand region. In: Nairn, A.E.M., Stehli, F.G., Uyeda, S. (Eds.), The Oceanic Basins and Margins. The Pacific Ocean, vol. 7B. Plenum Press, New York, pp. 411–482.

Leat, P.T., Storey, B.C., Pankhurst, R.J., 1993. Geochemistry of Paleozoic–Mesozoic Pacific rim orogenic magmatism, Thur-

ston Island area, West Antarctica. Antarctic Science 5 (3), 281–296.

Little, T.A., Mortimer, N., McWilliams, M., 1999. An episodic Cretaceous cooling model for the Otago-Marlborough Schist, New Zealand, based on Ar-40/Ar-39 white mica ages. New Zealand Journal of Geology and Geophysics 42 (3), 305–325.

Luyendyk, B., Cisowski, S., Smith, C., Richard, S., Kimbrough, D., 1996. Paleomagnetic study of the northern Ford Ranges, Western Marie Byrd Land, West Antarctica: motion between West and East Antarctica. Tectonics 15 (1), 122–141.

Luyendyk, B.P., 1995. Hypothesis for Cretaceous rifting of east Gondwana caused by subducted slab capture. Geology 23, 373–376.

MacKinnon, T.C., 1980. Sedimentologic, petrographic, and tectonic aspects of Torlesse and related rocks. Unpublished PhD thesis, University of Otago, Dunedin, New Zealand.

MacKinnon, T., 1983. Origin of the Torlesse terrane and coeval rocks, South Island, New Zealand. Geological Society of America Bulletin 94, 967–985.

Mazengarb, C., Harris, D.H.M., 1994. Cretaceous stratigraphic and structural relations of the Raukumara Peninsula, New Zealand: stratigraphic patterns associated the migration of a thrust system. Annales Tectonicae VIII, 100–118.

McCarron, J.J., Larter, R.D., 1998. Late Cretaceous to early Tertiary subduction history of the Antarctic Peninsula. Journal of the Geological Society of London 155 (Part 2), 255–268.

McDonough, W.F., Sun, S.S., Ringwood, A.E., Jagoutz, E., Hofmann, A.W., 1992. Potassium, rubidium, and cesium in the Earth and Moon and the evolution of the mantle of the Earth. In: McLennan, M.S., Rudnick, R. (Eds.), The Taylor Colloquium: Origin and Evolution of Planetary Crusts. Pergamon, Oxford, pp. 1001–1012.

McLennan, S.M., Hemming, S., 1992. Samarium/neodymium elemental and isotopic systematics in sedimentary rocks. Geochimica et Cosmochimica Acta 56, 887–898.

McLennan, S.M., Taylor, S.R., McCulloch, M.T., Maynard, J.B., 1990. Geochemical and Nd–Sr isotopic composition of deep-sea turbidites: crustal evolution and plate tectonic associations. Geochimica et Cosmochimica Acta 54 (7), 2015–2050.

Mildenhall, D.C., 1977. Cretaceous palynomorphs from the Waihere Bay Group and Kahuiatara Tuff, Chatham Island, New Zealand. New Zealand Journal of Geology and Geophysics 20, 655–672.

Millar, I.L., Willan, R.C.R., Wareham, C.D., Boyce, A.J., 2001. The role of crustal and mantle sources in the genesis of granitoids of the Antarctic Peninsula and adjacent crustal blocks. Journal of the Geological Society, London 2001 (5), 855–867.

Moore, G.W. et al., 1982. Plate-tectonic map of the circum-Pacific region. Circum-Pacific Map Project. The American Association of Petroleum Geologists, Tulsa, Oklahoma 74101, U.S.A.

Mortimer, N., 1993. Jurassic tectonic history of the Otago Schist, New Zealand. Tectonics 12 (1), 237–244.

Mortimer, N., 1995. Origin of the Torlesse terrane and coeval rocks, North Island, New Zealand. International Geology Review 36, 891–921.

Mortimer, N., et al., 1995. Ferrar magmatic province rocks discovered in New Zealand: implications for Mesozoic Gondwana geology. Geology 23 (2), 185–188.

Mortimer, N., Gans, P., Calvert, A., Walker, N., 1999. Geology and thermochronometry of the east edge of the Median Batholith (Median Tectonic Zone): a new perspective on Permian to Cretaceous crustal growth of New Zealand. Island Arc 8 (3), 404–425.

Muir, R.J., Ireland, T.R., Weaver, S.D., Bradshaw, J.D., 1994. Ion microprobe U–Pb zircon geochronology of granitic magmatism in the Western Province of the South Island, New Zealand. Chemical Geology 113 (1–2), 171–189.

Muir, R.J., Weaver, S.D., Bradshaw, J.D., Eby, G.N., Evans, J.A., 1995. The Cretaceous Separation Point Batholith, New Zealand: granitoid magmas formed by melting of mafic lithosphere. Journal of the Geological Society, London 152 (Part 4), 689–701.

Muir, R.J., et al., 1997. SHRIMP U–Pb geochronology of Cretaceous magmatism in northwest Nelson-Westland, South Island, New Zealand. New Zealand Journal of Geology and Geophysics 40, 453–463.

Muir, R.J., et al., 1998. Geochronology and geochemistry of a Mesozoic magmatic arc system, Fiordland, New Zealand. Journal of the Geological Society, London 155 (Part 6), 1037–1052.

Mukasa, S.B., Dalziel, I.W.D., 2000. Marie Byrd Land, West Antarctica: evolution of Gondwana's Pacific margin constrained by zircon U–Pb geochronology and feldspar common-Pb isotopic compositions. Geological Society of America Bulletin 112, 611–627.

Münker, C., Cooper, R.A., 1997. The early Paleozoic Takaka Terrane, New Zealand, as part of the Australian/Antarctic Gondwana margin: new insights from the trace element and isotope geochemistry of Cambrian volcanics. In: Bradshaw, J.D., Weaver, S.D. (Eds.), Terrane Dynamics 97, International Conference on Terrane Geology, Christchurch, New Zealand. Canterbury University Press, Christchurch, New Zealand, pp. 124–127.

Nakamura, N., 1974. Determination of REE, Ba, Fe, Mg, Na, and K in carbonaceous and ordinary meteorites. Geochimica et Cosmochimica Acta 38, 757–775.

Pankhurst, R.J., Millar, I.L., Grunow, A.M., Storey, B.C., 1993. The pre-Cenozoic magmatic history of the Thurston Island crustal block, West Antarctica. Journal of Geophysical Research B, Solid Earth and Planets 98 (7), 11835–11849.

Pankhurst, R.J., Weaver, S.D., Bradshaw, J.D., Storey, B.C., Ireland, T.R., 1998. Geochronology and geochemistry of pre-Jurassic superterranes in Marie Byrd Land, Antarctica. Journal of Geophysical Research B, Solid Earth and Planets 103 (B2), 2529–2547.

Pankhurst, R.J., Riley, T.R., Fanning, C.M., Kelley, S.P., 2000. Episodic silicic volcanism in Patagonia and the Antarctic Peninsula: chronology of magmatism associated with the break-up of Gondwana. Journal of Petrology 41 (5), 605–625.

Pearce, J.A., Harris, N.B.W., Tindle, A.G., 1984. Trace element discrimination diagrams for the tectonic interpretation of granitic rocks. Journal of Petrology 25, 956–983.

Peccerillo, A., Taylor, S.R., 1976. Geochemistry of Eocene calc-alkaline volcanic rocks from the Kastamonu area, northern Turkey. Contributions to Mineralogy and Petrology 58 (1), 63–81.

Pell, S.D., Williams, I.S., Chivas, A.R., 1997. The use of protolith zircon-age fingerprints in determining the protosource areas for some Australian dune sands. Sedimentary Geology 109, 233–260.

Pickard, A.L., Adams, C.J., Barley, M.E., 2000. Provenance of New Zealand Late Permian to Cretaceous depocentres at the Australian margin of Gondwanaland: evidence from detrital zircon SHRIMP dating. Australian Journal of Earth Sciences 47, 987–1007.

Powell, C.M., Li, Z.X., 1994. Reconstruction of the Panthalassan margin of Gondwanaland. In: Veevers, J., Powell, M. (Eds.), Permian–Triassic Pangean basins and foldbelts along the Panthalassan margin of Gondwanaland. Memoir-Geological Society of America. Geological Society of America (GSA), Boulder, CO, USA, pp. 5–9.

Raine, J.I., Strong, C.P., Wilson, G.J., 1993. Biostratigraphic revision of petroleum exploration wells, Great South Basin, New Zealand. Institute of Geological and Nuclear Sciences Science Report 93/32 (146 pp.).

Riley, T.R., Leat, P.T., Pankhurst, R.J., Harris, C., 2001. Origins of large volume rhyolitic volcanism in the Antarctic Peninsula and Patagonia by crustal melting. Journal of Petrology 42 (6), 1043–1065.

Roser, B.P., 1986. Chemistry, provenance and tectonic setting of New Zealand greywacke terranes. In: Anonymous (Editor), Geological Society of New Zealand, 16th annual conference; programme and abstracts. Geological Society of New Zealand Miscellaneous Publication. Geological Society of New Zealand, Christchurch, New Zealand, p. 88.

Roser, B.P., Korsch, R.J., 1988. Provenance signatures of sandstone–mudstone suites determined using discriminant function analysis of major-element data. Chemical Geology 67, 119–139.

Roser, B.P., Korsch, R.J., 1999. Geochemical characterization, evolution and source of a Mesozoic accretionary wedge: the Torlesse terrane, New Zealand. Geological Magazine 136 (5), 493–512.

Roser, B.P. et al., 2000. Whole-rock analyses of sandstones, siltstones, and tuffs from the Murihiku terrane, New Zealand. Research Report 7. Victoria University of Wellington, School of Earth Sciences, Wellington, New Zealand, 26 pp.

Silberling, N.J., Nichols, K.M., Bradshaw, J.D., Blome, C.D., 1988. Limestone and chert in tectonic blocks from the Esk Head subterrane, South Island, New Zealand. Geological Society of America Bulletin 100, 1213–1223.

Sircombe, K.N., 1999. Tracing provenance through the isotope ages of littoral and sedimentary detrital zircons, Eastern Australia. Sedimentary Geology 124, 47–67.

Smale, D., 1978. The composition of a Torlesse conglomerate: Ethelton, North Canterbury. New Zealand Journal of Geology and Geophysics 21 (6), 699–711.

Smale, D., 1997. Heavy minerals in the Torlesse terrane of the Wellington area, New Zealand. New Zealand Journal of Geology and Geophysics 40 (4), 499–506.

Speden, I.G., 1974. Additional fossil localities of the Torlesse rocks of the South Island (including summations of faunal assemblages and lithological information). New Zealand Geological Survey Report, vol. 69. Institute of Geological and Nuclear Sciences, Lower Hutt, New Zealand. 37 pp.

Spell, T.L., McDougall, I., Tulloch, A.J., 2000. Thermochronologic constraints on the breakup of the Pacific Gondwana margin: the Paparoa metamorphic core complex, South Island, New Zealand. Tectonics 19 (3), 433–451.

Storey, B.C., Hole, M.J., Pankhurst, R.J., Miller, I.L., Vennum, W., 1988. Middle Jurassic within-plate granites in West Antarctica and their bearing on the break-up of Gondwanaland. Journal of the Geological Society, London 145 (Part 6), 999–1007.

Storey, B.C., et al., 1999. Mantle plumes and Antarctica–New Zealand rifting; evidence from Mid-Cretaceous mafic dykes. Journal of the Geological Society, London 156 (Part 4), 659–671.

Stump, E., White, A.J.R., Borg, S.G., 1986. Reconstruction of Australia and Antarctica: evidence from granites and recent mapping. Earth and Planetary Science Letters 79 (3–4), 348–360.

Sutherland, R., 1999. Basement geology and tectonic development of the greater New Zealand region: an interpretation from regional magnetic data. Tectonophysics 308 (3), 341–362.

Tera, F., Wasserburg, G.J., 1972. U–Th–Pb systematics in three Apollo 14 basalts and the problem of initial Pb in lunar rocks. Earth and Planetary Science Letters 14, 281–304.

Tranter, T.H., 1992. Underplating of an accretionary prism: an example from the LeMay Group of central Alexander Island, Antarctic Peninsula. Journal of South American Earth Sciences 6 (1–2), 1–20.

Tulloch, A.J., 1983. Granitoid rocks of New Zealand: a brief review. In: Roddick, J.A. (Ed.), Circum-Pacific Plutonic Terranes. Memoir-Geological Society of America. Geological Society of America (GSA), Boulder, CO, USA, pp. 5–20.

Tulloch, A.J., Kimbrough, D.L., 1989. The Paparoa metamorphic core complex, New Zealand; Cretaceous extension associated with fragmentation of the Pacific margin of Gondwana. Tectonics 8 (6), 1217–1235.

Tulloch, A.J., Kimbrough, D.L., Landis, C.A., Mortimer, N., Johnston, M.R., 1999. Relationships between the Brook Street Terrane and Median Tectonic Zone (Median Batholith): evidence from Jurassic conglomerates. New Zealand Journal of Geology and Geophysics 42 (2), 279–293.

Van Der Plas, L., Tobi, A.C., 1965. A chart of judging the reliability of point counting results. American Journal of Science 263, 87–90.

Waight, T.E., et al., 1997. Field characteristics, petrography, and geochronology of the Hohonu Batholith and the adjacent Granite Hill Complex, North Westland, New Zealand. New Zealand Journal of Geology and Geophysics 40 (1), 1–17.

Waight, T.E., Weaver, S.D., Maas, R., Eby, G.N., 1998a. French Creek Granite and Hohonu dyke swarm, South Island, New Zealand: late Cretaceous alkaline magmatism and the opening of the Tasman Sea. Australian Journal of Earth Sciences 45 (6), 823–835.

Waight, T.E., Weaver, S.D., Muir, R.J., Maas, R., Eby, G.N., 1998b. The Hohonu Batholith of North Westland, New Zealand; Granitoid compositions controlled by source H_2O contents and generated during tectonic transition. Contributions to Mineralogy and Petrology 130 (3–4), 225–239.

Weaver, S.D., Pankhurst, R.J., 1991. A precise Rb–Sr age for the Mandamus Igneous complex, North Canterbury, and regional tectonic implications. New Zealand Journal of Geology and Geophysics 34, 341–345.

Weaver, S.D., Gibson, I.L., Houghton, B.F., Wilson, C.J., 1990. Mobility of rare earth and other elements during crystallisation of alkaline silicic lavas. Journal of Volcanology and Geothermal Research 43, 57–70.

Weaver, S.D., et al., 1994. Antarctica–New Zealand rifting and Marie Byrd Land lithospheric magmatism linked to ridge subduction and mantle plume activity. Geology 22 (9), 811–814.

Weaver, S.D., et al., 1996. Cretaceous Magmatism, make-up and break-up of the SW Pacific Gondwana margin. Mesozoic Geology of the Eastern Australia Plate Conference. Geological Society of Australia, Brisbane, p. 548.

Wombacher, F., Münker, K., 2000. Pb, Nd, and Sr Isotopes and REE systematics of Cambrian sediments from New Zealand: implications for the reconstruction of the Early Paleozoic Gondwana margin along Australia and Antarctica. The Journal of Geology 108, 663–686.

Wood, R., 1994. Geophysical aspect of the opening of the Tasman Sea. In: van der Lingen, G.J., Swanson, K.M., Muir, R.J. (Eds.), Evolution of the Tansman Sea Basin. Balkema, Rotterdam, pp. 19–34.

Wysoczanski, R.J., Gibson, G.M., Ireland, T.R., 1997. Detrital zircon age patterns and provenance in Late Paleozoic Early Mesozoic New Zealand; Terranes and development of the Paleo-Pacific Gondwana margin. Geology 25 (10), 939–942.